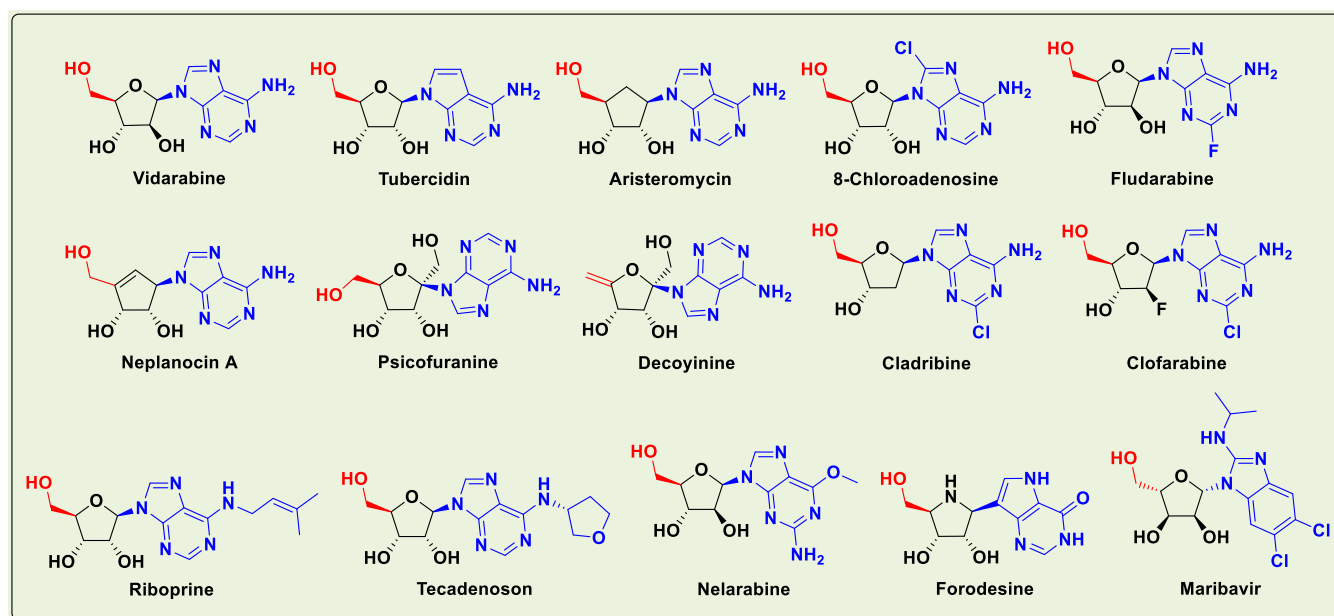


A



B

Figure 1. Chemical structures of: (A) Reference anti-SARS-CoV-2 drugs, remdesivir and molnupiravir, and their active TP metabolites, GS-443902 and NHC-TP, respectively. (B) Investigated NAs as potential anti-SARS-CoV-2 drugs (a small designed library).

first three examples reached to the clinical use stage successfully to date (only against the mild-to-moderate COVID-19 cases).^{8–15}

The mysterious SARS-CoV-2 Omicron variant, also known as B.1.1.529 (or BA), first began its tear around the world in late 2021 and now has more than three sisters of BA sublineages, e.g., BA.1, BA.2, and BA.3.²¹ South African scientists reported the new variant on November 24, 2021, immediately after its first appearance.²¹ As of January 7, 2022, the World Health Organization (WHO) reports that this highly infectious and virulent variant had been detected in

more than 150 countries.²¹ The Omicron variant has at least 36 new mutations in its spike (S) proteins.²² Being unfixed and changeable day by day from one strain to the newer, spike protein is not an attractive target for designing new therapies against SARS-CoV-2 variants. However, on the other hand, targeting the universal fixed proteins among all variants, e.g., SARS-CoV-2 replication RNA-dependent RNA polymerase (RdRp) and proofreading 3'-to-5' exoribonuclease (ExoN) enzymes, through repurposing known compounds is a much more effective and time-saving approach in this battle, even against the expectedly coming resistant SARS-CoV-2 strains.

Table 1. Binding Affinity Energy Values (Docking S-Scores) Estimated during Molecular Docking of the 15 Screened TP Nucleotides of the Corresponding 15 Target NAs against the Two SARS-CoV-2 Proteins, RdRp and ExoN Enzymes (Using GS-443902 and NHC-TP as the Positive Control Drugs)^a

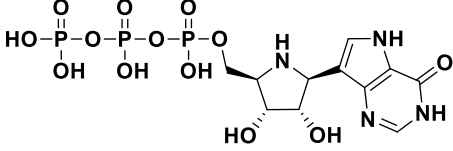
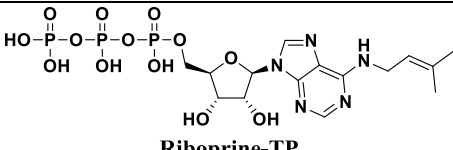
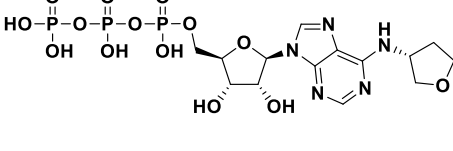
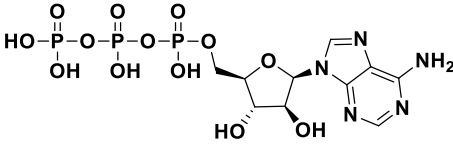
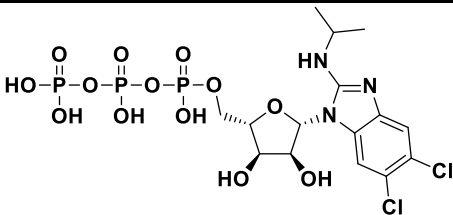
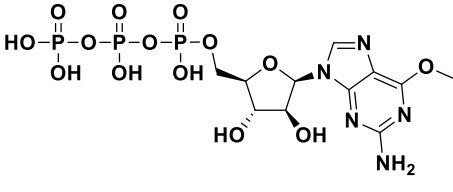
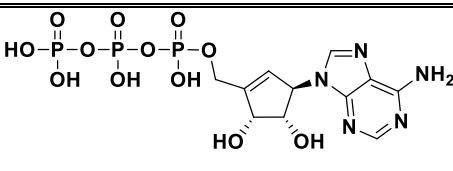
Classification	TP Compound	Docking S-score (kcal/mol)	
		RdRp (7BV2)	ExoN (7MC6)
<i>Screened Nucleotide Analogues of the Target Drugs</i>	 <p>Forodesine-TP</p>	-7.1	-8.7
	 <p>Riboprime-TP</p>	-7.1	-7.9
	 <p>Tecadenoson-TP</p>	-6.8	-8.2
	 <p>Vidarabine-TP</p>	-6.7	-7.9
	 <p>Maribavir-TP</p>	-7.1	-7.3
	 <p>Nelarabine-TP</p>	-7.0	-7.1
	 <p>Neplanocin-A-TP</p>	-6.6	-7.5

Table 1. continued

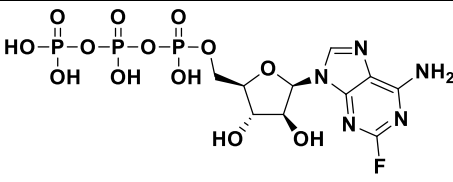
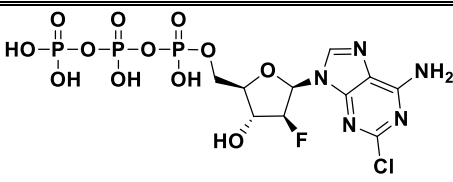
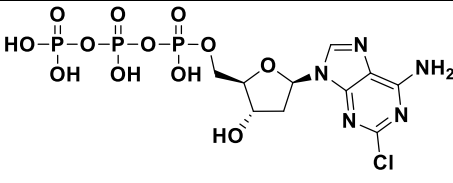
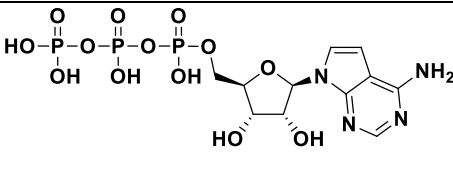
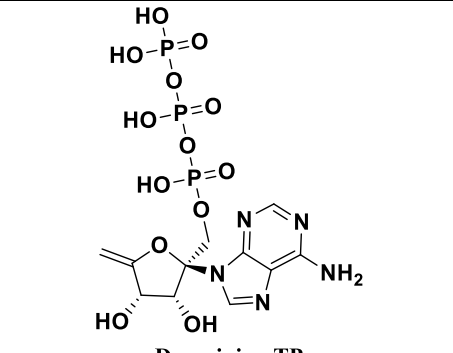
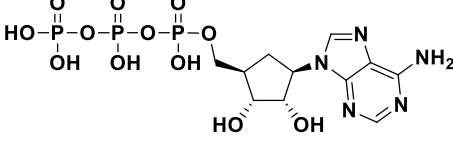
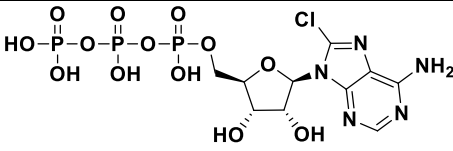
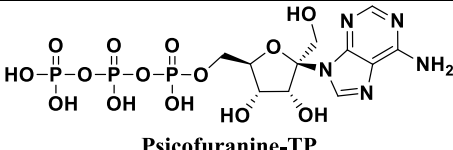
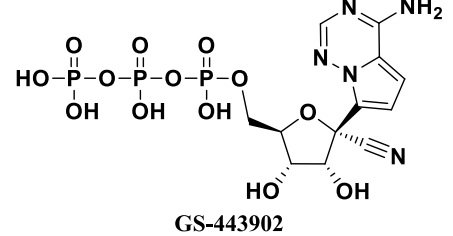
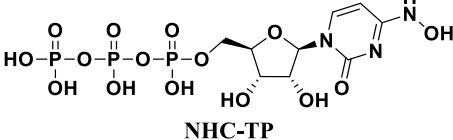
Classification	TP Compound	Docking S-score (kcal/mol)	
		RdRp (7BV2)	ExoN (7MC6)
	 <p>Fludarabine-TP</p>	-6.4	-7.6
	 <p>Clofarabine-TP</p>	-6.3	-7.7
	 <p>Cladribine-TP</p>	-6.8	-7.1
	 <p>Tubercidin-TP</p>	-6.4	-7.5
	 <p>Decoyinine-TP</p>	-6.4	-7.3
	 <p>Aristeromycin-TP</p>	-6.1	-7.6

Table 1. continued

Classification	TP Compound	Docking S-score (kcal/mol)	
		RdRp (7BV2)	ExoN (7MC6)
	 8-Chloroadenosine-TP	-6.3	-7.3
	 Psicofuranine-TP	-6.0	-7.6
Screened Active Nucleotide Metabolites of the Reference Drugs	 GS-443902	-7.0	-7.8
	 NHC-TP	-6.4	-7.5

^aThe 15 TP nucleotides are arranged in a collective descending order, beginning from the top-ranked one and ending with the least-ranked one.

Moreover, therapies targeting the spike protein have only one chance to fight the coronaviral infection since after the passage of any viral particles inside the host body (or if these therapies were taken after the occurrence of the infection) there will not be any further abilities of these therapies to stop virus propagation and infection. Unlike therapies targeting the replication and proofreading enzymes, which have an unlimited number of continuous chances to fight the virus and its successors, and prevent their further multiplication throughout the entire human body (even if these therapies were taken after the occurrence of the infection). In the first weeks of 2022, we as a multidisciplinary team continued our scientific journey and worked around the clock to discover effective anti-SARS-CoV-2 Omicron variant drug candidates.

Tactical nucleos(t)ide analogism is among the favorable therapeutic choices in drug designers' and pharmaceutical chemists' brains to fight and stop the coronavirus multiplication inside the human body.^{9–15,20} In this COVID-19 therapeutic tactic, the used nucleoside/nucleotide analogue makes use of its close similarity to the normal natural nucleosides and nucleotides to misguide and deceive the SARS-CoV-2 RdRp (the nonstructural protein complex 12/7/8 or nsp12–nsp7–nsp8) and ExoN (the nonstructural protein complex 14/10 or nsp14–nsp10) enzymes.²⁰ Nsp12–nsp7–nsp8 and nsp14–nsp10 protein complexes are very indispensable enzymes in the replication/proofreading of the SARS-CoV-2 genome, and thus, their strong inhibition will significantly block the replication of SARS-CoV-2 particles.

Nucleoside-like agents confuse both RdRp and ExoN enzymes through complete incorporation in the viral RNA genetic strands in place of the correct naturally occurring nucleosides/nucleotides, resulting in repeated excessive ambiguous coding and premature termination of RNA synthesis with the formation of vague RNA strands at the end; these faulty strands represent abnormal noninfectious and inactive particles; hence, there would not be any further multiplication of the virus.^{13,14,20} Some of the aforementioned anti-COVID-19 agents, e.g., remdesivir and molnupiravir and their final active triphosphate (TP) metabolites, GS-443902 and β -D-N⁴-hydroxycytidine 5'-TP (NHC-TP), respectively (Figure 1A), draw on this effective mechanism in their inhibitory and blocking activities on the SARS-CoV-2 particles.^{9–12} With the progressive evolution of more resistant new strains/variants of SARS-CoV-2, discovering more potent and broad-spectrum natural or synthetic anti-SARS-CoV-2 drugs became a must.

In this current research work, we have explored the combined inhibitory activities of some NAs on both SARS-CoV-2 RdRp and ExoN enzymes as a novel effective strategy to doubly combat COVID-19.²³ After screening different libraries of nucleosides and NAs, we chose the top 15 nucleoside-like compounds with the best results to make a very small library of them specifically designed for our work (Figure 1B). Another small library (TP Nucleotide Library) was created from the active TP nucleotides corresponding to the previous 15 NAs (see their structures in Table 1). Computation-based molecular docking revealed that about

six of these corresponding 15 nucleotides showed very good binding free energies with both enzymes, SARS-CoV-2 RdRp and ExoN, compared to those of the two positive TP nucleotide controls (references), GS-443902 and NHC-TP, with the same two enzymes. However, the other compounds of the 15 ones, e.g., neplanocin-A-TP, fludarabine-TP, and clofarabine-TP, showed relatively moderate to good results. Molecular docking and dynamics simulations studies of the chosen six compounds (in both the free nucleoside and TP nucleotide forms) disclosed the superiority of the two compounds forodesine and riboprine and their corresponding TP nucleotides in hitting the catalytic active sites of both enzymes with the formation of much more stable complexes having higher negative binding free energies. Biological evaluation of the original six NAs (the free nontriphosphorylated nucleosidic forms of the previously chosen TP nucleotides) against both SARS-CoV-2 RdRp and ExoN proteins and against the entire SARS-CoV-2 Omicron variant particles demonstrated nearly the same interesting therapeutic superiority of riboprine and forodesine. Accordingly, their TP nucleotides, riboprine-TP and forodesine-TP, were selected to be tested for the same collective anti-SARS-CoV-2 activities, revealing the expected promising clinical results of forodesine-TP and riboprine-TP, respectively.

Based on these current results and previous data,^{24–27} we can conclude that, first, riboprine and forodesine can be further *in vivo* and clinically investigated for repurposing against COVID-19 and, second, the expected potent clinical inhibitory effects of riboprine and forodesine against SARS-CoV-2 replication may be mainly attributed to the double synergistic inhibitory activities against the two enzymes RdRp and ExoN, i.e., may be closely related to the RdRp/ExoN inhibitory activities of riboprine and forodesine. The possible SARS-CoV-2 RNA mutagenicity of both drugs *via* nucleoside/nucleotide analogism mode of action and incorporation into the new SARS-CoV-2 RNA strands should also be extensively and clinically studied. The pharmacokinetics of these drugs that we intend to try repurposing against COVID-19 should be significantly taken into account because tissue distributions of these potential anti-SARS-CoV-2 drugs will certainly affect their total capabilities of reducing viral loads of SARS-CoV-2 particles in COVID-19 therapy.²⁸ The possibility of pharmaceutically formulating the current promising six nucleoside-like agents (or their corresponding TP nucleotide agents) as rapid-action nasal/oral anti-COVID-19 spray/drops and/or in combination therapies should also be considered.

2. MATERIALS AND METHODS

2.1. *In Silico* Computational Evaluation

2.1.1. Preparation of Targeted SARS-CoV-2 Proteins. The three-dimensional (3D) structures of the targeted SARS-CoV-2 RdRp and ExoN proteins were obtained from the RCSB Protein Data Bank (PDB) with PDB identification codes 7BV2 and 7MC6, respectively. Both enzymatic proteins were obtained in the complex forms with their protein cofactors (i.e., were obtained cocrystallized in the nsp12–nsp7–nsp8 and nsp14–nsp10 complex forms, respectively) to simulate the natural status. The PDB files of the two proteins were properly downloaded. Proteins were viewed through Pymol Molecular Graphic Visualizer software 2.4, and their pre-detected active site residues (with their closest neighboring residues) were then checked for complete presence and correctness. The catalytic active site residues highlighted through Pymol software were noted for the next *in silico* studies.

2.1.2. Selection and Preparation of Nucleosidic/Nucleotidic Ligands. To choose the best TP nucleotides for the current study, primary virtual screening of diverse libraries of hundreds of NAs was done against SARS-CoV-2 RdRp and ExoN proteins using the Molecular Operating Environment (MOE) platform (Chemical Computing Group). The 15 NAs with the top collective results as the best hitting candidates of both proteins were selected to continue the long procession of this current research study. After this precise screening, an extensive literature survey was also performed for the study of the potential of the chosen 15 NAs as antivirals. Many of them have demonstrated strong antiviral capabilities either in computational or experimental studies or in both of them. This is one of the main reasons we have tried these potential inhibitors and their active metabolic TP ester forms in the current virtual docking and simulation studies of SARS-CoV-2 RdRp and ExoN enzymes. The chemical structures of the selected NAs and their corresponding TP nucleotides were accurately prepared using ChemDraw Professional 16.0 software (licensed version) for the next *in silico* studies.

2.1.3. Molecular Docking Protocol. Blind docking of the 15 selected TP nucleotides in SARS-CoV-2 RdRp and ExoN proteins was done *via* MOE. Two reference anti-SARS-CoV-2 RdRp/ExoN TP nucleotides GS-443902 and NHC-TP were used as positive controls in this methodology. Prior to starting these docking procedures, some important preparations (mainly, additions and corrections) are required. All of the missed atoms/residues in the SARS-CoV-2 RdRp and ExoN were added *via* MOE structure modeling. The two specific proteins were precisely prepared for molecular docking by the addition of hydrogen atoms using the 3D protonation module of the used MOE software; any partial charges were also corrected for both proteins. RdRp and ExoN were energy-minimized in their complex forms *via* the Amber-99 force field, which is available in MOE. Similarly, the structures of the 15 target nucleotidic ligands, GS-443902, and NHC-TP were also adequately energy-minimized in MOE. For docking of the target/reference ligands with the two proteins, the known London-dG scoring functions were utilized for binding energy calculations. For each docked target/reference molecule, the MOE software produced about 20 different poses with each docked SARS-CoV-2 protein. Of all docking poses for each molecule with each protein, the one with the highest number of best molecular interactions, i.e., the top-ranked pose or the best interactions, was recorded and saved. MOE gives a numerical value for the interaction of any potential ligand with any certain protein in the form of docking S-score (docking scores are expressed in kcal/mol). This docking binding energy or S-score represents the net energy of the formed protein–ligand complex and it also primarily reflects the degree of its expected stability (i.e., it provides a primary idea about the predicted stability of this formed complex prior to performing the more detailed robust computations *via* the molecular dynamics “MD” simulations). The molecular docking revealed six promising target nucleotides with very good S-scores compared to the two reference nucleotides (these six top-ranked active nucleotides and their original nucleoside prodrugs represent the central point of the current research). MOE software shows all of the possible molecular interactions (of all types) made during the docking process; these include, e.g., hydrogen-bonding (H-bond) interactions, hydrophobic interactions, ionic interactions/bonds, and salt bridges. For the best six target nucleotides and the two potent reference nucleotides, the two-dimensional (2D) and 3D output images of all of the produced protein–ligand complexes (showing almost all of the possible interactions) were saved for reporting and further investigative analysis.

2.1.4. Molecular Dynamics (MD) Simulation Protocol. The six TP nucleotides ranked with the top results, e.g., with the best molecular interactions, lowest docking score (S-score), and lowest root-mean-square deviation (RMSD), computed through MOE and the apoenzyme against both proteins were then employed for further *in silico* studies, mainly the MD simulation studies, using Schrodinger’s Desmond module MD Simulation software. For MD simulations of the selected nucleotides, the best docking poses of these nucleotides in complexes with the SARS-CoV-2 RdRp and

ExoN enzymes were kept in PDB format in MOE to be used for further virtual stability studies in Schrodinger's Desmond module. The in-built Desmond System Builder tool was used in this current protocol to create a solvated water-soaked MD Simulation system. The TIP3P model was utilized as the solvating model in the present experiment. With periodic boundary conditions, an orthorhombic box was accurately simulated with a good boundary distance of at least 10 Å from the outer surface of each of the two SARS-CoV-2 proteins. The simulation systems were neutralized of complex charges by the addition of a reasonably sufficient amount of counter ions. The isosmotic state was maintained by adding 0.10 mol/L sodium and chloride ions, i.e., 0.10 M NaCl, into the simulation panel to keep isosmotic conditions. Prior to beginning the simulation process, a predefined equilibration procedure was done. The system of the MD simulation was equilibrated by employing the standard Desmond protocol at a constant pressure of 1.0 bar and a constant temperature of 300 K (NPT ensemble; considering the viral nature of the two targeted enzymatic proteins) and also by employing the known Berendsen coupling protocol with one temperature group. Hydrogen atom bond length was properly constrained using the validated SHAKE algorithm. The particle mesh Ewald (PME) summation method was used to specifically model long-range electrostatic interactions. On the other hand, an exact cutoff of 10 Å was specifically assigned for van der Waals and short-range electrostatic interactions. As previously mentioned, the MD simulation was run at ambient pressure conditions of about 1.013 bar, while the used temperature was exactly set to 300 K for each 100 ns period of this MD simulation, and 1000 frames were saved into the simulation trajectory file. The simulation run time for each complex system and apo system was fixed to 100 ns in total. After simulations, the trajectory file of the simulated system was used for the calculation of the various structural parameters required, e.g., RMSD (Å), root-mean-square fluctuation (RMSF; Å), radius of gyration (rGyr; Å), number of protein–ligand contacts (# of total contacts), interactions fractions (%), intermolecular H-bonds (from all aspects), molecular surface area (MolSA; Å²), solvent-accessible surface area (SASA; Å²), and polar surface area (PSA; Å²), to extensively perform stability studies of the complex and apo systems. The results of the most promising two nucleotidic compounds, forodesine-TP and riboprime-TP, were saved to be reported and discussed in the current paper.

2.2. In Vitro Biological Evaluation

2.2.1. Specifications of the Bioassayed NAs and TP Nucleotide Analogues. Riboprime (*N*⁶-(2-Isopentenyl)adenosine, CAS registry number 7724-76-7) was purchased from BenchChem (BENCH CHEMICAL, Austin, Texas, U.S.A.) (catalog number B141774, purity ≥99%). While forodesine (ImmuCellin-H, CAS registry number 209799-67-7), nelarabine (Arranon, CAS registry number 121032-29-9), tecadenoson (CVT-510, CAS registry number 204512-90-3), maribavir (1263W94, CAS registry number 176161-24-3), vidarabine (Arabinosyladenine “Ara-A”, CAS registry number 5536-17-4), remdesivir (GS-5734, CAS registry number 1809249-37-3), and molnupiravir (EIDD-2801, CAS registry number 2349386-89-4) were purchased from Biosynth Carbosynth (Carbosynth Ltd., Berkshire, U.K.) (for forodesine, product code MD11591, purity ≥98%; for nelarabine, product code NN26176, purity ≥98%; for tecadenoson, product code EIA51290, purity ≥98%; for maribavir, product code AM178224, purity ≥98%; for vidarabine, product code NA06007, purity ≥98%; for remdesivir, product code AG170167, purity ≥98%; for molnupiravir, product code AE176721, purity ≥98%). The ultrapure solvent dimethylsulfoxide (DMSO, CAS registry number 67-68-5) was purchased from a local distributor, El-Gomhouria Company For Drugs (El-Gomhouria Co. For Trading Drugs, Chemicals & Medical Supplies, Mansoura Branch, Egypt) (purity ≥99.9% “anhydrous”). Forodesine-TP and riboprime-TP were purchased from Biosynth Carbosynth and BENCH CHEMICAL, respectively, through custom synthesis contracts. GS-443902 (as trisodium salt, CAS registry number 1355050-21-3) was purchased from Biosynth Carbosynth (Carbosynth Ltd., Berkshire, U.K.) (product code FEC05021, purity ≥95%). While NHC-TP (EIDD-

1931-TP, CAS registry number 34973-27-8) was purchased from MedChemExpress (MCE, MedChemExpress LLC, New Jersey, U.S.A.) (catalog number HY-135867, purity 98.02%).

2.2.2. In Vitro Anti-RdRp/Anti-ExoN Assay (SARS-CoV-2 RdRp-Gluc Reporter Assay) of the Selected NAs and TP Nucleotide Analogues. First, the used cells, 293T cells (ATCC CRL-3216), were kept in Dulbecco's modified Eagle's medium (DMEM; Gibco) with 10% (v/v) fetal bovine serum (FBS; Gibco); then, they were cultured at 37 °C in a humidified atmosphere of CO₂ (5%). HEK293T cells were transfected using Vigofect transfection reagents (Vigorous) according to the strict instructions of the manufacturer. The required plasmid DNAs, antibodies, and reagents were purchased and treated exactly as in the literature procedures.^{24,25} The tested drugs are as described and specified in Section 2.2.1. Also, western blotting (for the collected transfected HEK293T cells), real-time polymerase chain reaction (RT-PCR, for the extracted total RNA of transfected HEK293T cells), and cell viability test (using Cell Counting Kit-8 (CCK8), Beyotime) were exactly performed as the typical literature methods.^{24,25} The steps of the well-designed *in vitro* SARS-CoV-2-RdRp-Gluc reporter assay were accurately carried out according to the same original method of literature but with almost all of the proteins modified and relevant to the SARS-CoV-2 Omicron variant “B.1.1.529.1/BA.1 sublineage” (HEK293T cells were transfected in this biochemical assay with CoV-Gluc, nsp12, nsp7, and nsp8 plasmid DNAs at a ratio of 1:10:30:30 and with CoV-Gluc, nsp12, nsp7, nsp8, nsp10, and nsp14 plasmid DNAs at a ratio of 1:10:30:30:10:90).^{24,25} Exactly as instructed in the original assay, a stock of coelenterazine-h was dissolved in absolute ethanol (of very pure analytical grade) to a concentration of 1.022 mM.^{24,25} Directly before each assay, the stock was diluted in phosphate-buffered saline (PBS) to a concentration of 16.7 μM and incubated in the dark for 30 min at room temperature.^{24,25} For the luminescence assay, 10 μL of supernatant was added to each well of a white and opaque 96-well plate, then 60 μL of 16.7 μM coelenterazine-h was injected, and luminescence was measured for 0.5 s using a Berthold Centro XS3 LB 960 microplate luminometer.^{24,25} The primary results showed that riboprime and forodesine are the top-ranked NAs among the six target ones; thus, we chose their corresponding TP nucleotide analogues, riboprime-TP and forodesine-TP, to be also similarly tested. Both nucleotides underwent the same procedures/steps, exactly as mentioned above (using the two TP nucleotides GS-443902 and NHC-TP as the positive control/reference drugs instead, and similarly DMSO as the negative control/placebo drug). The final results were statistically represented as the mean (μ) ± standard deviation (SD) from at least three independent experiments. Statistical analysis was performed using SkanIt 4.0 Research Edition software (Thermo Fisher Scientific) and Prism V5 software (GraphPad). All resulting data were considered statistically significant at $p < 0.05$.

2.2.3. In Vitro Anti-SARS-CoV-2 and Cytotoxic Bioactivities Multiassay of the Selected NAs and TP Nucleotide Analogues. This validated *in vitro* anti-COVID-19 multiassay (including the cytotoxicity test), which was designed for the assessment of the net anti-SARS-CoV-2 activities of potential anti-COVID-19 agents, is based mainly upon the authentic procedures of Rabie.^{5,13,14,16–19} The complete procedures were carried out in a specialized biosafety level 3 (BSL-3) laboratory upon safety approval. The assayed new strain of SARS-CoV-2 virus, the Omicron variant, B.1.1.529.1/BA.1 sublineage, was isolated from the fresh nasopharynx aspirate and throat swab of a 47.5-year-old Chinese man with confirmed COVID-19 infection using Vero E6 cells (ATCC CRL-1586) on June 1, 2022. The starting titer of the stock virus ($10^{7.25}$ TCID₅₀/mL) was prepared after three serial passages in Vero E6 cells in infection media (DMEM supplemented with 4.5 g/L D-glucose, 100 mg/L sodium pyruvate, 2% FBS, 100 000 U/L penicillin–streptomycin, and 25 mM *N*-(2-hydroxyethyl)-piperazine-*N'*-ethanesulfonic acid (HEPES)). The tested target and reference NAs are as described and specified in Section 2.2.1. Preliminary pilot assays were performed mainly to determine the best concentration of the tested NAs to begin the *in vitro* anti-SARS-CoV-2 and cytotoxicity tests. Accordingly, the stocks of the tested

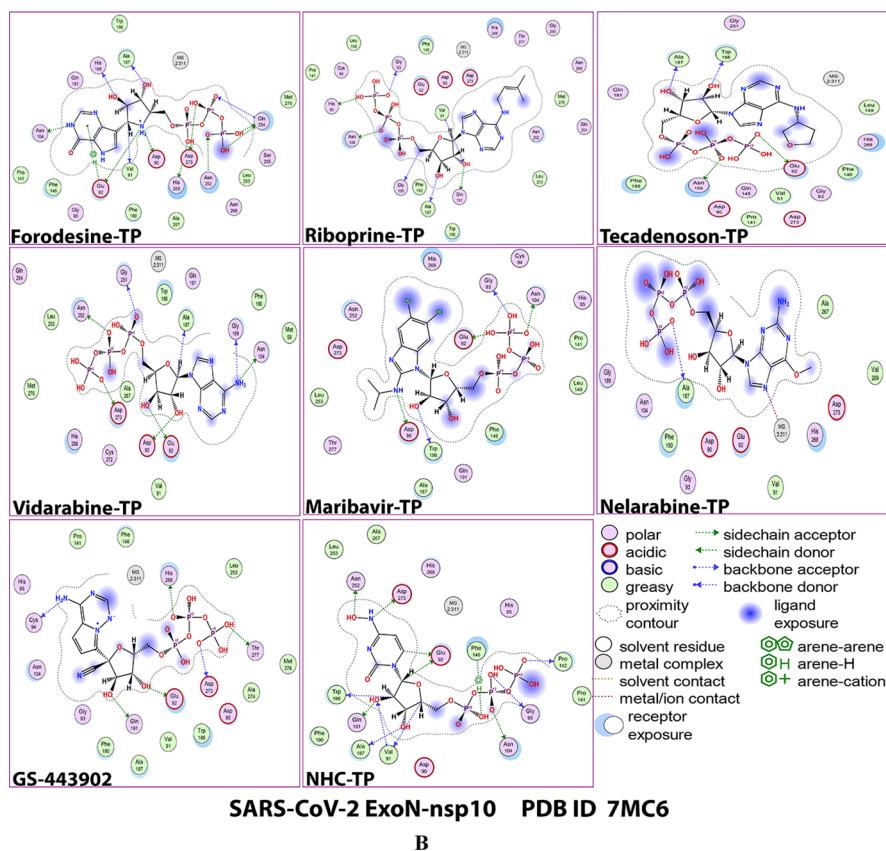
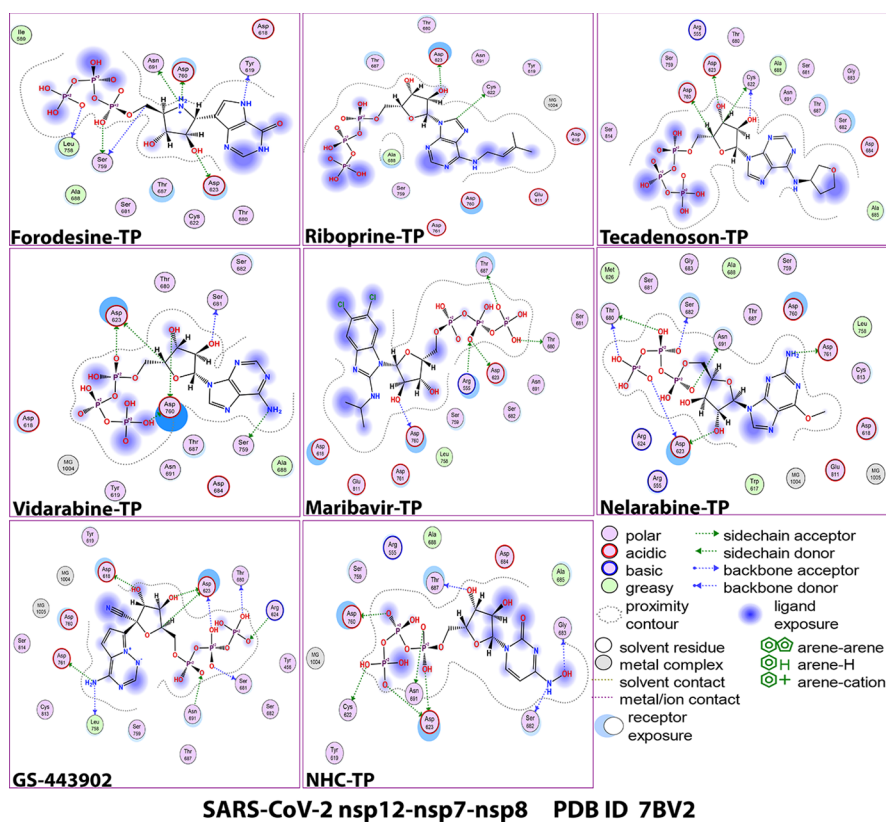


Figure 2. 2D images of the postdocking interactions of the six TP nucleotide analogues, forodesine-TP, riboprine-TP, tecadenoson-TP, vidarabine-TP, maribavir-TP, and nelarabine-TP, and the two reference TP nucleotide analogue drugs, GS-443902 and NHC-TP, respectively, with: (A) SARS-CoV-2 RdRp “nsp12” enzyme cocrystallized with its protein cofactors nsp7 and nsp8 (PDB ID: 7BV2). (B) SARS-CoV-2 ExoN “nsp14” enzyme cocrystallized with its protein cofactor nsp10 (PDB ID: 7MC6).

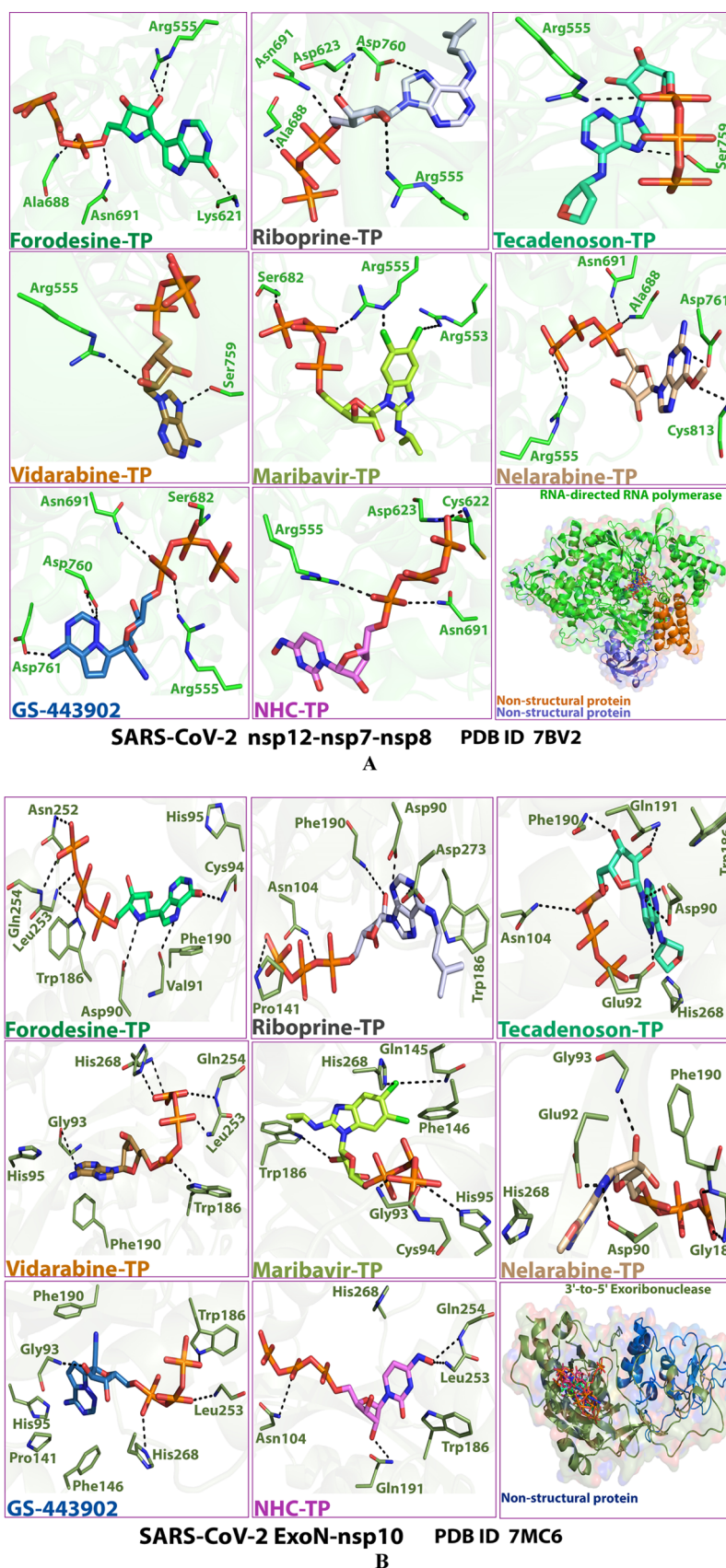


Figure 3. 3D images of the postdocking interactions of the six TP nucleotide analogues, forodesine-TP, riboprine-TP, tecadenoson-TP, vidarabine-TP, maribavir-TP, and nelarabine-TP, and the two reference TP nucleotide analogue drugs, GS-443902 and NHC-TP, respectively, with: (A) SARS-CoV-2 RdRp “nsp12” enzyme cocrystallized with its protein cofactors nsp7 and nsp8 (PDB ID: 7BV2). (B) SARS-CoV-2 ExoN “nsp14” enzyme cocrystallized with its protein cofactor nsp10 (PDB ID: 7MC6).

compounds were precisely prepared by dissolving each of the eight compounds in DMSO to obtain a 100 μM concentration of each compound. Additionally, DMSO was used for the purpose of a negative control comparison to make this experimental study placebo-controlled. To assess the total *in vitro* anti-SARS-CoV-2 activity of each of the target drugs, riboprine, forodesine, nelarabine, tecadenoson, maribavir, and vidarabine, in comparison to that of each of the two positive control/reference drugs, remdesivir and molnupiravir, along with that of the negative control solvent, DMSO, Vero E6 cells were pretreated with each of the nine compounds diluted in infection media for 1 h prior to infection by the new Omicron variant of the SARS-CoV-2 virus at MOI = 0.02. The nine tested compounds were maintained with the virus inoculum during the 2 h incubation period. The inoculum was removed after incubation, and the cells were overlaid with infection media containing the diluted test compounds. After 48 h of incubation at 37 $^{\circ}\text{C}$, supernatants were immediately collected to quantify viral loads by the TCID₅₀ assay or quantitative real-time RT-PCR “qRT-PCR” (TaqMan Fast Virus 1-Step Master Mix). Viral loads in this assay were fitted on a logarithm scale (\log_{10} TCID₅₀/mL, \log_{10} TCID₉₀/mL, and \log_{10} viral RNA copies/mL), not on a linear scale, under increasing concentrations of the tested compounds. Four-parameter logistic (4PL) regression (GraphPad Prism) was used to fit the dose–response curves and determine the EC₅₀ and EC₉₀ of the tested compounds that inhibit SARS-CoV-2 viral replication (CPEIC₁₀₀ was also determined for each compound). Cytotoxicity of each of the nine tested compounds was also evaluated in Vero E6 cells using the CellTiter-Glo Luminescent Cell Viability Assay (Promega). The primary results showed that riboprine and forodesine are the top-ranked NAs among the six target ones; thus, we chose their corresponding TP nucleotide analogues, riboprine-TP and forodesine-TP, to be also similarly tested. Both nucleotides underwent the same procedures/steps, exactly as above mentioned (using the two TP nucleotides GS-443902 and NHC-TP as the positive control/reference drugs instead, and similarly DMSO as the negative control/placebo drug). The final results were statistically represented as $\mu \pm \text{SD}$ from at least three independent experiments. Statistical analysis was done using SkanIt 4.0 Research Edition software (Thermo Fisher Scientific) and Prism V5 software (GraphPad). All produced data were considered statistically significant at $p < 0.05$.

3. RESULTS AND DISCUSSION

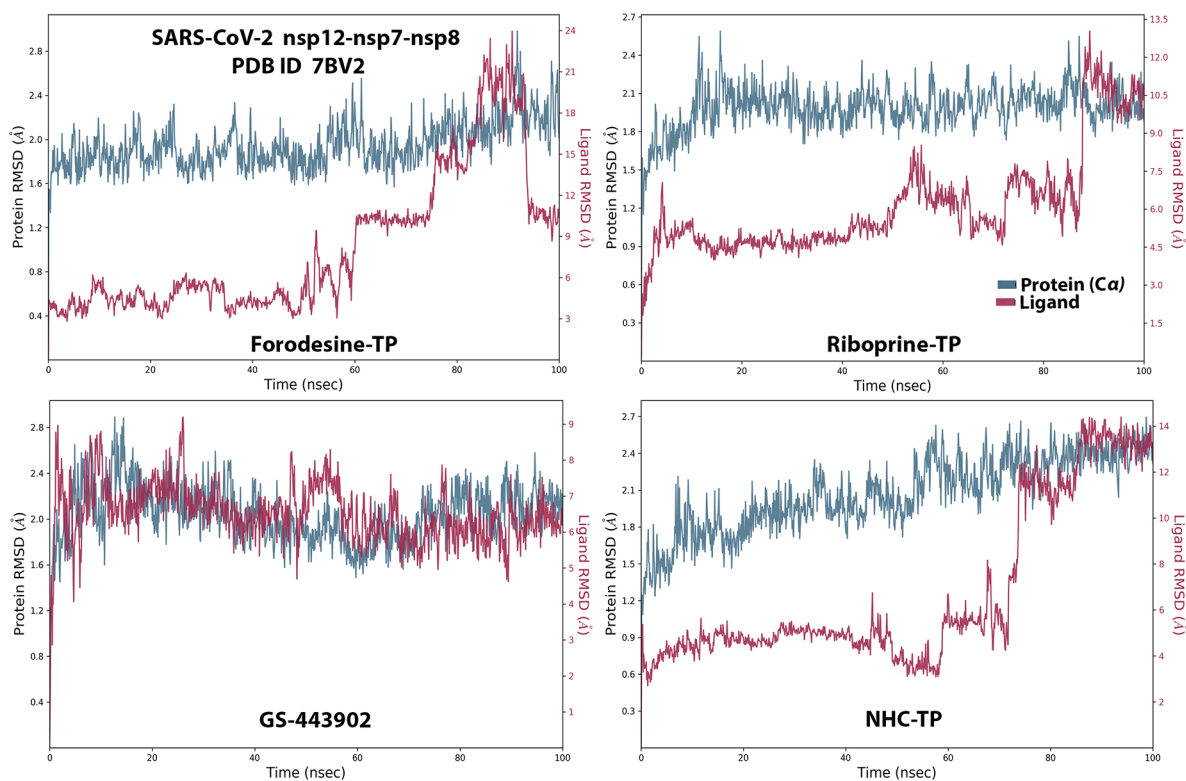
3.1. Computational Molecular Modeling of the Selected NAs and TP Nucleotide Analogues as Potential Anti-COVID-19 Drugs

After computational screening and filtration of several libraries of nucleosides and NAs, the top 15 nucleoside-like molecules with the best and most ideal pharmacodynamic/pharmacokinetic results with respect to the predicted anti-SARS-CoV-2 activities were selected for our targeted work. The chosen compounds are, respectively, as follows: forodesine, riboprine, tecadenoson, vidarabine, maribavir, nelarabine, neplanocin-A, fludarabine, clofarabine, cladribine, tubercidin, decoyinine, aristeromycin, 8-chloroadenosine, and psicofuranine. A small new library was made of these 15 compounds, which are a mixture of natural and synthetic molecules (Figure 1B). A second small new library was consequently designed from the TP nucleotide analogues of the 15 target compounds; this is also to computationally investigate the target NAs in their final active TP nucleotide forms (which are the predominant active forms in the *in vivo*/clinical environments). In the next step, further molecular docking specifically against SARS-CoV-2 RdRp and ExoN revealed that the nucleotide compounds forodesine-TP, riboprine-TP, tecadenoson-TP, vidarabine-TP, maribavir-TP, and nelarabine-TP, respectively, have the lowest and best inhibitory binding energies (ranging from -6.7 to

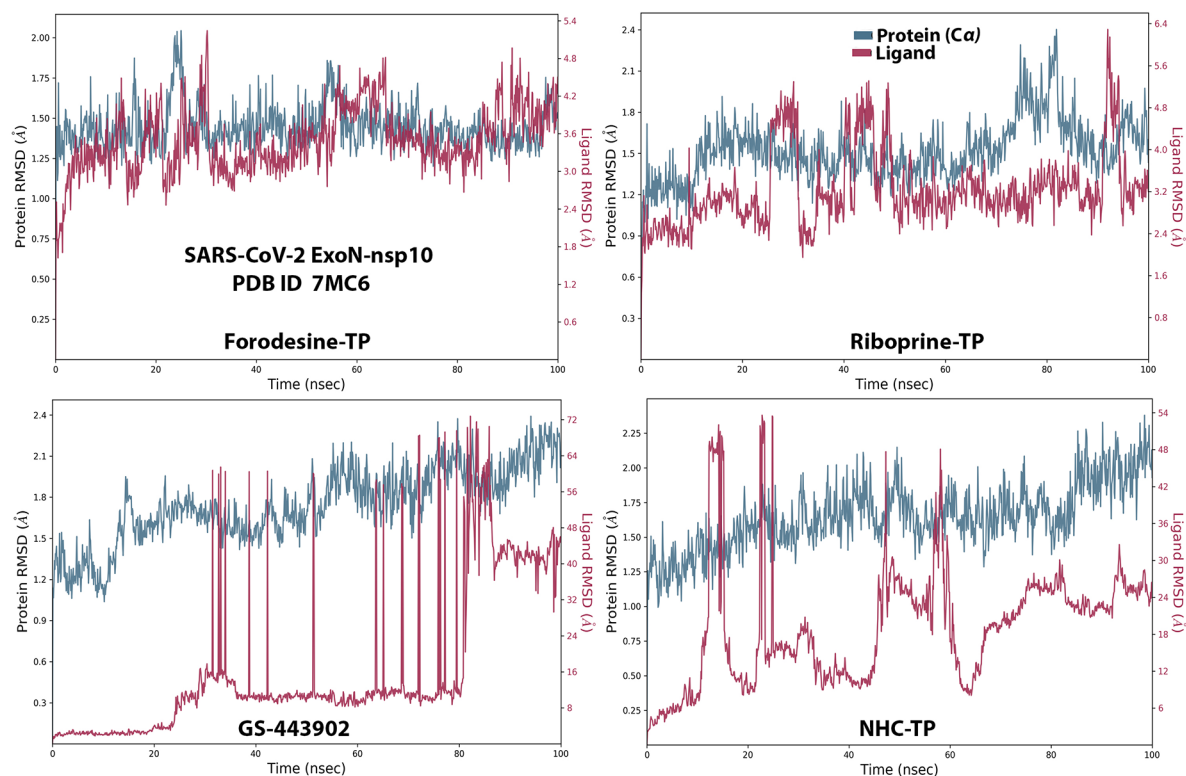
-8.7 kcal/mol) compared to the two reference anti-RdRp/anti-ExoN nucleotide drugs, GS-443902 and NHC-TP (having binding energies ranging from -6.4 to -7.8 kcal/mol), as shown in Table 1. The catalytic pockets (i.e., active sites) of the two SARS-CoV-2 enzymes, RdRp (which is the main enzyme responsible for replication and transcription of the SARS-CoV-2 RNA genome) and ExoN (it is worth mentioning that nsp14 or the proofreading exoribonuclease of SARS-CoV-2 has two active sites; the exoribonuclease active site, the major one that we are concerned with in the current study, and the methyltransferase active site), were nearly detected and validated through previous several computational, crystallographic, and biochemical experiments in the literature.^{29–32} Investigating and analyzing the resulting *in silico* interactions of the aforementioned six molecules with the residues of SARS-CoV-2 RdRp and ExoN proteins showed that all molecules effectively hit and interact with most of the active amino acid residues of the catalytic pockets of both enzymes with strong interactions, including, mainly, H-bonding interactions, hydrophobic interactions, ionic bonding, and water bridges (weaker in some examples), of relatively short bond distances and low binding energies.

Figures 2A,B and 3A,B show the detailed 2D and 3D representations of the most apparent intermolecular interactions between each ligand of the six ones with each of the two SARS-CoV-2 enzymes, respectively. The 3D representations focus mostly on the shortest bonds. The molecules of the target six TP nucleotide analogues strongly strike most of the neighboring active residues of the major catalytic pocket of SARS-CoV-2 RdRp (in chain A, i.e., 7BV2-A receptor), e.g., Arg553, Arg555, Ile589, Trp617, Asp618, Tyr619, Lys621, Cys622, Asp623, Arg624, Met626, Thr680, Ser681, Ser682, Gly683, Asp684, Thr687, Ala688, Asn691, Leu758, Ser759, Asp760, Asp761, Glu811, Cys813, and Ser814. On the other hand, the molecules of the same six nucleotide analogues powerfully make interactions with most of the adjacent active residues of the major catalytic pocket (exoribonuclease active site) of SARS-CoV-2 ExoN (in chain A; QHD43415_13 receptor), e.g., Met58, Asp90, Val91, Glu92, Gly93, Cys94, His95, Asn104, Pro141, Gln145, Phe146, Leu149, Trp186, Ala187, His188, Gly189, Phe190, Gln191, Gly251, Asn252, Leu253, Gln254, Ser255, Asn266, His268, Asp273, and Thr277. These interactions are very favorable and very comparable to, or even in some cases significantly better than, those of GS-443902 and NHC-TP with the same two enzymes.

Analysis of the MD simulation results revealed the relatively good stabilities of the formed protein–ligand complexes of each of the six TP nucleotide analogue with each of the two enzymes when compared with the two reference ligands. Complexes of the TP nucleotide analogues with SARS-CoV-2 ExoN are much more stable, with less numbers/intensities of fluctuations, and with lower RMSD (\AA) and RMSF (\AA) values than those with SARS-CoV-2 RdRp. Interestingly, forodesine-TP and riboprine-TP displayed the best results among all in most of the compared MD items during the simulation. Comprehensively, the RdRp–forodesine-TP, RdRp–riboprine-TP, ExoN–forodesine-TP, and ExoN–riboprine-TP complexes appeared to be reasonably stable. The early fluctuations (which were not mostly drastic) in RMSF and RMSD trajectories may be indications of some conformational changes within the enzyme complex system as a result of the adequate repositioning of both target ligands inside the



A



B

Figure 4. RMSD trajectories (during a simulation period of 100 ns) of the α -carbon of amino acid residues of the protein (blue color) and the ligand (maroon color) in the protein–ligand complexes of the two TP nucleotide analogues, forodesine-TP and riboprime-TP, and the two reference TP nucleotide analogue drugs, GS-443902 and NHC-TP, respectively, with: (A) SARS-CoV-2 RdRp “nsp12” enzyme cocrystallized with its protein cofactors nsp7 and nsp8 (PDB ID: 7BV2). (B) SARS-CoV-2 ExoN “nsp14” enzyme cocrystallized with its protein cofactor nsp10 (PDB ID: 7MC6).

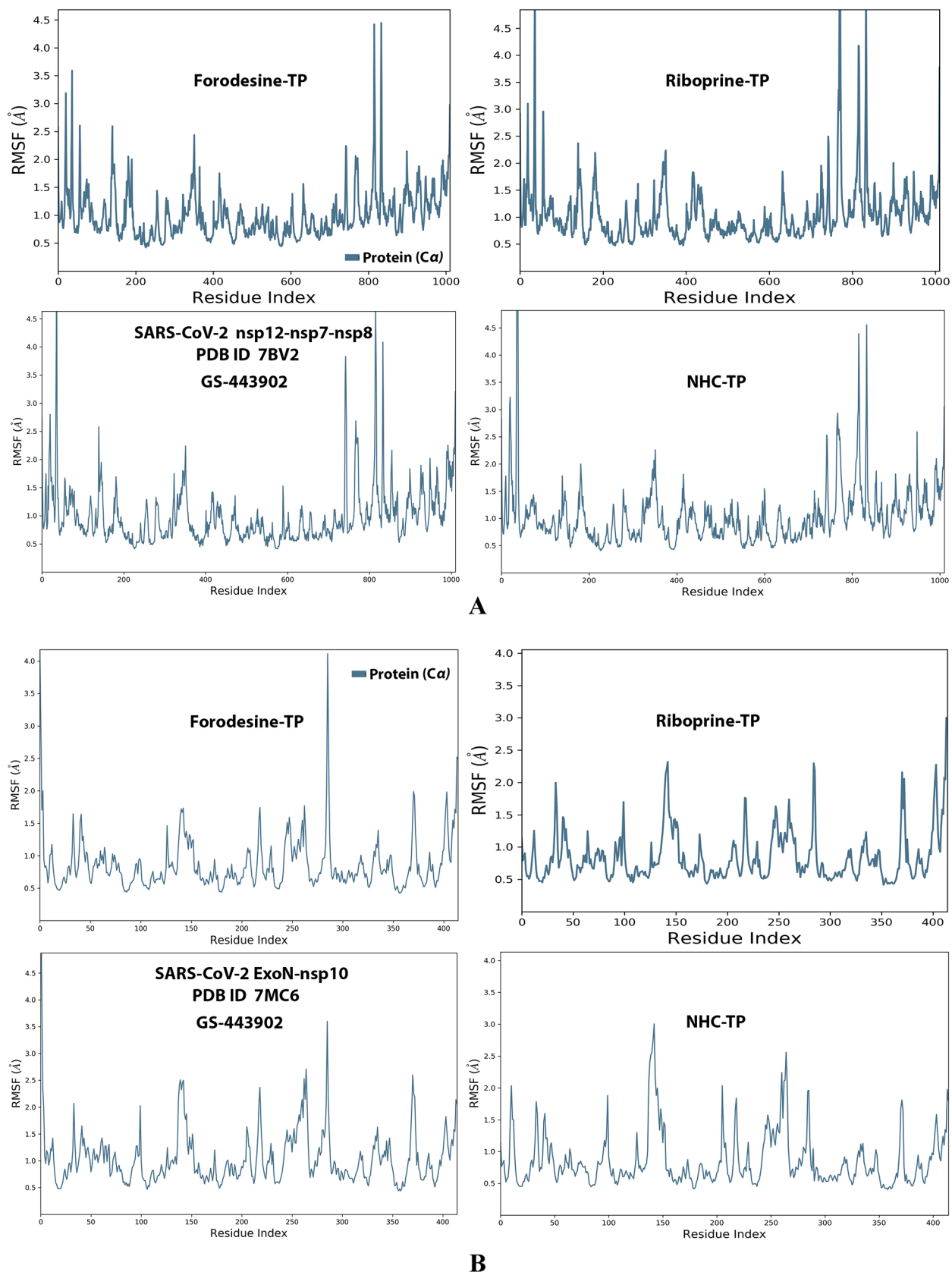


Figure 5. RMSF trajectories (along the different residue regions) of the α -carbon of amino acid residues of the protein in the protein–ligand complexes of the two TP nucleotide analogues, forodesine-TP and riboprine-TP, and the two reference TP nucleotide analogue drugs, GS-443902 and NHC-TP, respectively, with: (A) SARS-CoV-2 RdRp “nsp12” enzyme cocrystallized with its protein cofactors nsp7 and nsp8 (PDB ID: 7BV2) and (B) SARS-CoV-2 ExoN “nsp14” enzyme cocrystallized with its protein cofactor nsp10 (PDB ID: 7MC6).

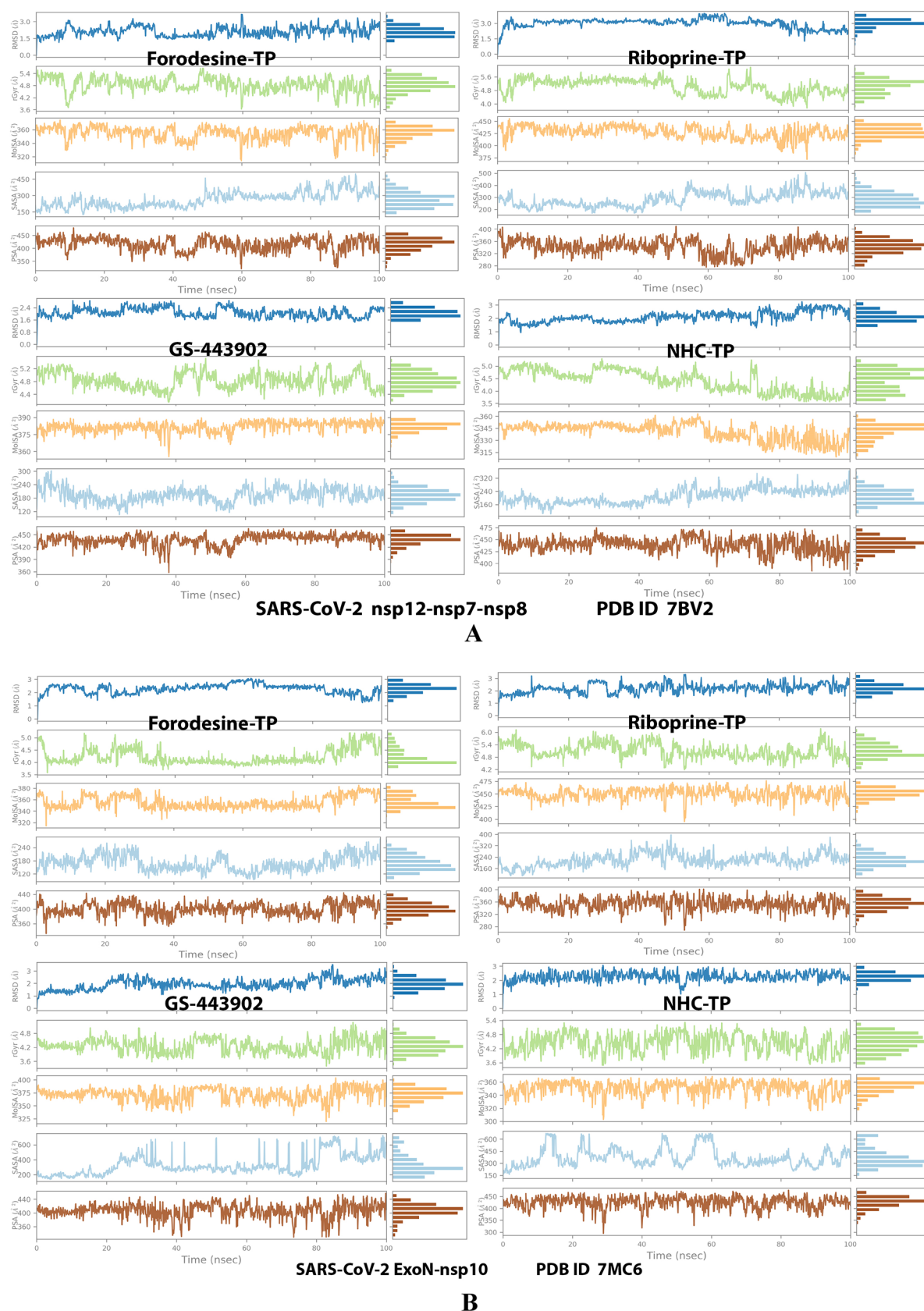


Figure 6. Collective post-MD simulation analysis of the protein–ligand complexes properties (RMSD, rGyr, MolSA, SASA, and PSA) of the two TP nucleotide analogues, forodesine-TP and riboprine-TP, and the two reference TP nucleotide analogue drugs, GS-443902 and NHC-TP, respectively, with: (A) SARS-CoV-2 RdRp “nsp12” enzyme cocrystallized with its protein cofactors nsp7 and nsp8 (PDB ID: 7BV2). (B) SARS-CoV-2 ExoN “nsp14” enzyme cocrystallized with its protein cofactor nsp10 (PDB ID: 7MC6).

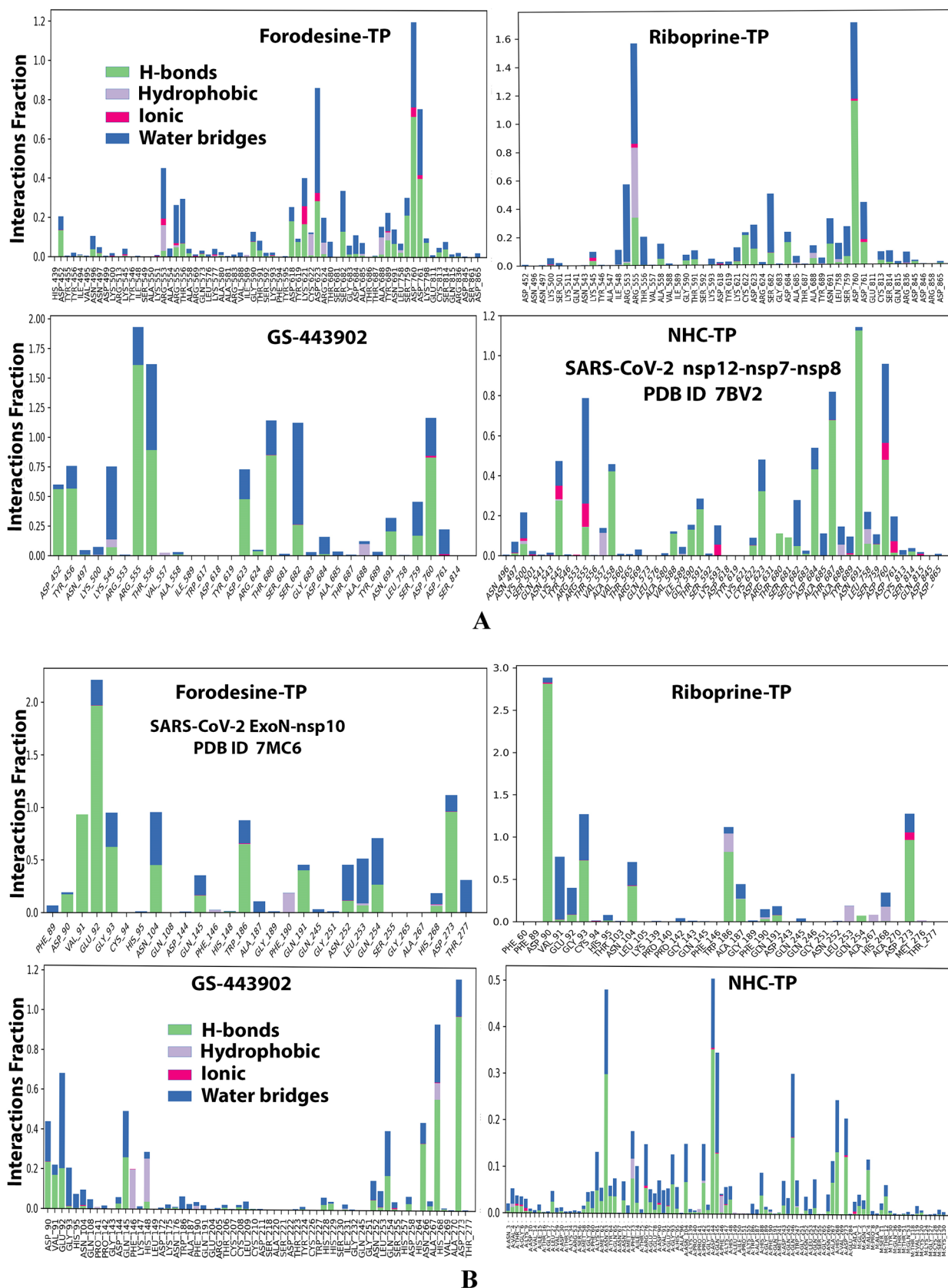


Figure 7. Histograms of the protein–ligand interactions fractions throughout the simulative interaction trajectories of the two TP nucleotide analogues, forodesine-TP and riboprine-TP, and the two reference TP nucleotide analogue drugs, GS-443902 and NHC-TP, respectively, with: (A) SARS-CoV-2 RdRp “nsp12” enzyme cocrystallized with its protein cofactors nsp7 and nsp8 (PDB ID: 7BV2). (B) SARS-CoV-2 ExoN “nsp14” enzyme cocrystallized with its protein cofactor nsp10 (PDB ID: 7MC6).

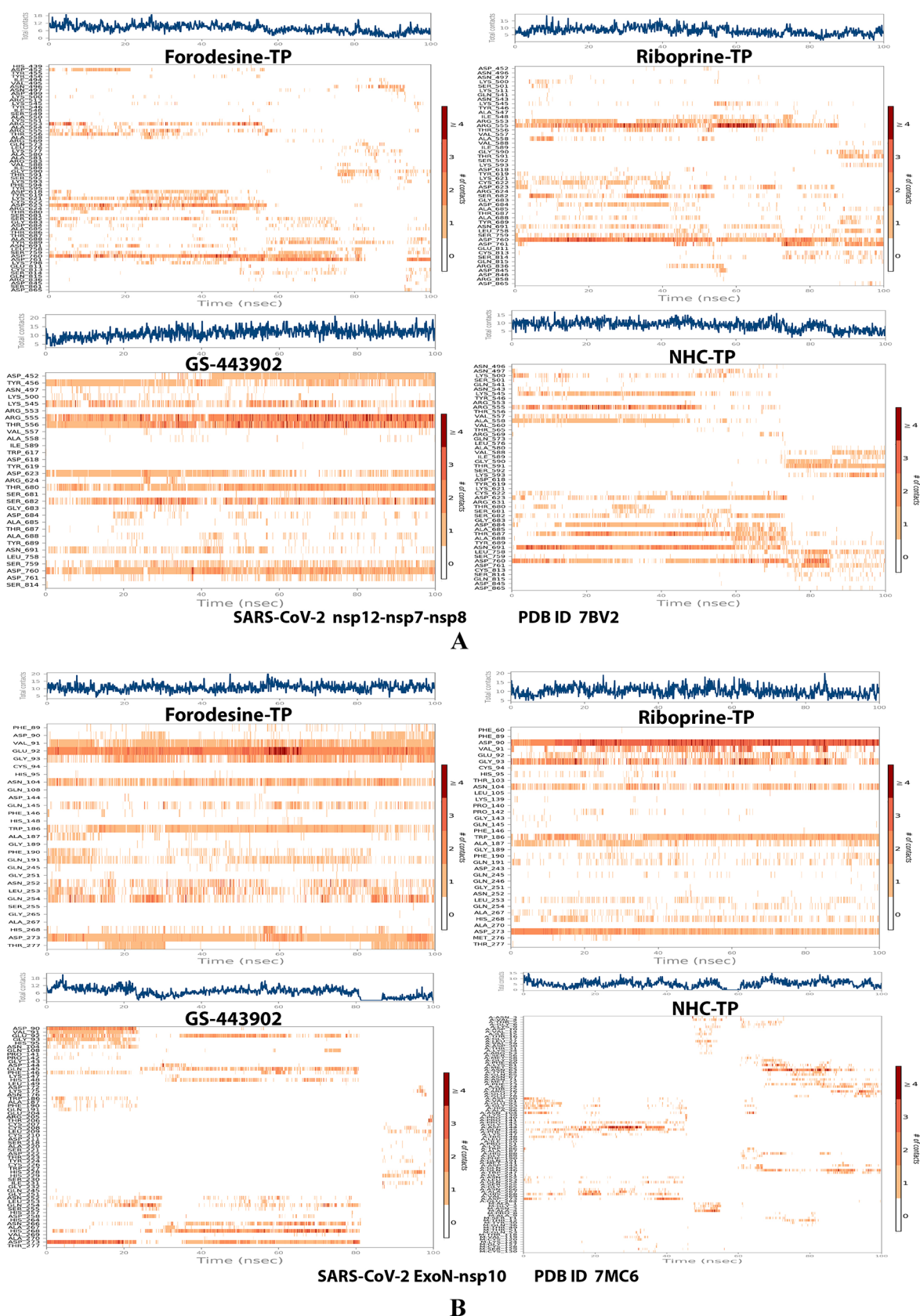


Figure 8. Plots of the distribution of the total number of interactions (contacts) in each trajectory framework of the protein–ligand complexes of the two TP nucleotide analogues, forodesine-TP and riboprine-TP, and the two reference TP nucleotide analogue drugs, GS-443902 and NHC-TP, respectively, with: (A) SARS-CoV-2 RdRp “nsp12” enzyme cocrystallized with its protein cofactors nsp7 and nsp8 (PDB ID: 7BV2). (B) SARS-CoV-2 ExoN “nsp14” enzyme cocrystallized with its protein cofactor nsp10 (PDB ID: 7MC6).

Table 2. Anti-SARS-CoV-2 RdRp/ExoN Activities (along with Respective Ratios) of the Target Repurposed Drugs Riboprine, Forodesine, Nelarabine, Tecadenoson, Maribavir, and Vidarabine (Using Both Remdesivir and Molnupiravir as the Positive Control/Reference Drugs and DMSO as the Negative Control/Placebo Drug) and the TP Nucleotides Forodesine-TP and Riboprine-TP (Using Both GS-443902 and NHC-TP as the Positive Control/Reference Drugs and DMSO as the Negative Control/Placebo Drug), respectively, in HEK293T Cells, Expressed as EC₅₀ Values in μM (Please Note That, in This Table, nsp12 Refers to the nsp12/7/8 Complex, nsp14 Refers to the nsp14/10 Complex, and nsp14_{mutant} Refers to the nsp14_{mutant}/10 Complex)

classification	compound name	inhibition of SARS-CoV-2 RdRp <i>in vitro</i> (EC ₅₀ in μM) ^a			respective ratios of EC ₅₀	
		Nsp12	nsp12 + nsp14	nsp12 + nsp14 _{mutant}	(nsp12 + nsp14)/nsp12	(nsp12 + nsp14 _{mutant})/nsp12
repurposed NAs	riboprine	0.18 ± 0.02	0.28 ± 0.03	0.23 ± 0.02	1.56	1.28
	forodesine	0.20 ± 0.03	0.31 ± 0.03	0.25 ± 0.03	1.55	1.25
	nelarabine	0.65 ± 0.04	1.22 ± 0.06	1.09 ± 0.05	1.88	1.68
	tecadenoson	0.99 ± 0.06	1.38 ± 0.06	1.29 ± 0.04	1.39	1.30
	maribavir	1.07 ± 0.05	1.89 ± 0.07	1.45 ± 0.07	1.77	1.36
	vidarabine	1.08 ± 0.06	2.02 ± 0.08	1.47 ± 0.07	1.87	1.36
reference drugs	remdesivir	1.12 ± 0.06	2.11 ± 0.09	1.55 ± 0.07	1.88	1.38
	molnupiravir	0.24 ± 0.03	0.45 ± 0.05	0.33 ± 0.04	1.88	1.38
placebo solvent	DMSO	>100	>100	>100	N.A. ^b	N.A.
TP nucleotide forms of the top-ranked repurposed NAs	forodesine-TP	0.16 ± 0.02	0.25 ± 0.04	0.20 ± 0.02	1.56	1.25
	riboprine-TP	0.17 ± 0.02	0.27 ± 0.03	0.21 ± 0.03	1.59	1.24
active TP metabolites of the reference drugs	GS-443902	1.05 ± 0.05	2.01 ± 0.09	1.51 ± 0.06	1.91	1.44
	NHC-TP	0.23 ± 0.03	0.42 ± 0.05	0.31 ± 0.03	1.83	1.35

^aEC₅₀ or 50% effective concentration is the concentration of the tested compound that is required for 50% reduction in the COVID-19 polymerase (SARS-CoV-2 RdRp) activity *in vitro*. EC₅₀ is expressed in μM . ^bN.A. means not available (i.e., it was not determined).

catalytic binding sites, which takes some nanotime until the formation of very interesting strong molecular interactions. Possible unrevealed allosteric modulations, especially in the case of the larger protein complex SARS-CoV-2 nsp12–nsp7–nsp8, could also be put into consideration. Forodesine-TP and GS-443902 have the lowest rGyr values (almost less than 5.0 Å) among all of the four analyzed compounds, especially with the ExoN enzyme, indicating more compact and stable protein complex systems. Furthermore, from the computational point of view, forodesine-TP followed by riboprine-TP have good and balanced MolSA, SASA, and PSA values in their SARS-CoV-2 enzymatic complexes, which are very comparable to the corresponding values of the two reference compounds. Interestingly, riboprine-TP displayed the largest interactions fraction (of more than 2.8% of the total interactions predicted) of the strong H-bonds with the hit SARS-CoV-2 proteins, among all of the tested compounds, and this specifically occurs between its substituted adenine nucleobase and the catalytic amino acid residue ExoN-Asp90 in the relatively stable small ExoN–riboprine-TP complex (see Figure 3B, recall that riboprine and riboprine-TP are typical adenosine and adenosine triphosphate “ATP” analogues, respectively), indicating a significantly high potential of riboprine/riboprine-TP to give a strongly-inhibited/blocked status of the ExoN enzyme. Similarly, forodesine-TP gives the second top-ranked H-bonding interactions fraction (of about 2.0% of the total interactions predicted), but with the catalytic amino acid residue ExoN-Glu92 instead. The MD simulation results also confirmed nearly all of the primary molecular docking data with regard to, for example, the interacting amino acids along with the numbers/types/strengths of the formed bonds. Figures 4A,B, 5A,B, 6A,B, 7A,B, and 8A,B show the detailed results of the MD simulation of interactions between each TP nucleotide ligand (of the most promising two NAs, forodesine and riboprine) with each of the two SARS-CoV-2 enzymes,

RdRp and ExoN, respectively (in comparison with the two reference anti-SARS-CoV-2 RdRp nucleotide drugs, GS-443902 and NHC-TP). The previous computational data were very encouraging to motivate us to continue with the biological evaluation part of the current work.

3.2. Experimental Biological Evaluation of the Selected NAs and TP Nucleotide Analogues as Potential Anti-COVID-19 Drugs

The first preclinical assay in this extensive assessment is the robust cell-based test, the *in vitro* anti-SARS-CoV-2 RdRp bioassay, which was recently developed using Gaussia-luciferase (Gluc) as the reporter to assess the anti-SARS-CoV-2 RdRp/ExoN activities of mainly the nucleos(t)ide analogues.^{24,25} Moreover, it was undoubtedly confirmed, through the findings of this new biochemical assay, that the exonuclease activity of SARS-CoV-2 nsp14 significantly improves the SARS-CoV-2 RdRp resistance to the various inhibitors of the nucleos(t)ide analogue class (one of the primary factors that aggravate the resistance and severe pathogenicity of SARS-CoV-2 particles is their abilities to encode the nsp14 ExoN that is capable of taking off the faulty mutagenic nucleotides misincorporated by the low-fidelity RdRp into the growing SARS-CoV-2 RNA strands, causing considerable resistance to the therapeutic potentials of the nucleos(t)ide analogue agents); thus, ExoN effects were considered and added in the steps of this screening assay protocol that was primarily designed for exploring possible SARS-CoV-2 RdRp inhibitors (dissimilar to the traditional analytical cell-free assay).^{24,25,33,34} The assay can be metaphorically called “anti-SARS-CoV-2 RdRp/ExoN bioassay”.

As previously mentioned, we mainly concentrate here on the two principal protein complexes that catalyze and control the SARS-CoV-2 replication/transcription processes, nsp12–nsp7–nsp8 polymerase complex and nsp14–nsp10 exoribonuclease complex, respectively. This test significantly simulates

Table 3. Anti-SARS-CoV-2/Anti-COVID-19 Activities (along with Cytotoxicities) of the Target Repurposed Drugs Riboprine, Forodesine, Nelarabine, Tecadenoson, Maribavir, and Vidarabine (Using Both Remdesivir and Molnupiravir as the Positive Control/Reference Drugs and DMSO as the Negative Control/Placebo Drug) and the TP Nucleotides Forodesine-TP And Riboprine-TP (Using Both GS-443902 and NHC-TP as the Positive Control/Reference Drugs and DMSO as the Negative Control/Placebo Drug), respectively, against SARS-CoV-2 (Omicron Variant, B.1.1.529.1/BA.1 Sublineage) in Vero E6 Cells

classification	compound name	CC ₅₀ ^a (μM)	inhibition of SARS-CoV-2 replication <i>in vitro</i> (anti-B.1.1.529.1/BA.1 bioactivities) (μM)			
			100% CPE inhibitory concentration (CPEIC ₁₀₀) ^b	50% reduction in infectious virus (EC ₅₀) ^c	50% reduction in viral RNA copy (EC ₅₀) ^d	90% reduction in infectious virus (EC ₉₀) ^e
repurposed NAs	riboprine	>100	1.08 ± 0.04	0.40 ± 0.02	0.42 ± 0.02	1.50 ± 0.06
	forodesine	>100	1.58 ± 0.07	0.65 ± 0.03	0.69 ± 0.04	2.02 ± 0.07
	nelarabine	>100	4.12 ± 0.15	1.67 ± 0.08	1.76 ± 0.08	6.42 ± 0.19
	tecadenoson	>100	7.65 ± 0.25	2.86 ± 0.11	2.93 ± 0.12	11.89 ± 0.31
	maribavir	>100	7.99 ± 0.28	3.00 ± 0.13	3.14 ± 0.15	12.24 ± 0.33
	vidarabine	>100	8.05 ± 0.29	3.21 ± 0.12	3.25 ± 0.11	12.65 ± 0.36
reference drugs	remdesivir	>100	5.90 ± 0.26	2.01 ± 0.09	2.08 ± 0.10	7.97 ± 0.35
	molnupiravir	>100	6.24 ± 0.31	2.60 ± 0.11	2.71 ± 0.11	9.16 ± 0.37
placebo solvent	DMSO	>100	>100	>100	>100	>100
TP nucleotide forms of the top-ranked repurposed NAs	forodesine-TP	>100	1.02 ± 0.04	0.38 ± 0.02	0.41 ± 0.03	1.46 ± 0.06
	riboprine-TP	>100	1.06 ± 0.05	0.39 ± 0.03	0.43 ± 0.03	1.51 ± 0.07
active TP metabolites of the reference drugs	GS-443902	>100	4.88 ± 0.22	1.70 ± 0.08	1.82 ± 0.08	6.45 ± 0.29
	NHC-TP	>100	5.03 ± 0.25	2.14 ± 0.10	2.30 ± 0.11	7.89 ± 0.31

^aCC₅₀ or 50% cytotoxic concentration is the concentration of the tested compound that kills half the cells in uninfected cell culture. CC₅₀ was determined with serially diluted compounds in Vero E6 cells at 48 h postincubation using the CellTiter-Glo Luminescent Cell Viability Assay (Promega). ^bCPEIC₁₀₀ or 100% CPE inhibitory concentration is the lowest concentration of the tested compound that causes 100% inhibition of the cytopathic effects (CPE) of SARS-CoV-2 B.1.1.529.1/BA.1 virus in Vero E6 cells under increasing concentrations of the tested compound at 48 h postinfection. Compounds were serially diluted from 100 μM concentration. ^cEC₅₀ or 50% effective concentration is the concentration of the tested compound that is required for 50% reduction in infectious SARS-CoV-2 B.1.1.529.1/BA.1 virus particles *in vitro*. EC₅₀ is determined by infectious virus yield in culture supernatant at 48 h postinfection (log₁₀ TCID₅₀/mL). ^dEC₅₀ or 50% effective concentration is the concentration of the tested compound that is required for 50% reduction in SARS-CoV-2 B.1.1.529.1/BA.1 viral RNA copies *in vitro*. EC₅₀ is determined by viral RNA copies number in culture supernatant at 48 h postinfection (log₁₀ RNA copies/mL). ^eEC₉₀ or 90% effective concentration is the concentration of the tested compound that is required for 90% reduction in infectious SARS-CoV-2 B.1.1.529.1/BA.1 virus particles *in vitro*. EC₉₀ is determined by infectious virus yield in culture supernatant at 48 h postinfection (log₁₀ TCID₉₀/mL).

the respective original replication processes that occur for the SARS-CoV-2 genome, as it functionally mimics the RNA generating processes driven mainly by SARS-CoV-2 RdRp.³⁵ Table 2 displays the detailed values obtained from this *in vitro* anti-SARS-CoV-2 RdRp/ExoN bioassay. The resulting data showed that, among the tested target NAs, riboprine and forodesine demonstrated the best results. The two compounds effectively inhibited SARS-CoV-2 RdRp activity with very excellent small EC₅₀ values of 0.18 and 0.20 μM, which very slightly increased in the presence of SARS-CoV-2 ExoN (the wild type) to about 0.28 and 0.31 μM, respectively, indicating the potent inhibitory/blocking activities of both compounds against SARS-CoV-2 ExoN, which appeared in these extremely minute nanomolar differences of the EC₅₀ values between both cases. Mutations in the exoribonuclease (i.e., the mutated type; e.g., D90A/E92A mutations of the active catalytic residues in nsp14 as in our current case) reinforced the anti-RdRp activity of riboprine and forodesine to excellent EC₅₀ values of 0.23 and 0.25 μM, respectively (i.e., slightly lower than that resulted in the presence of the normal wild type of ExoN; these very slight changes also reflected, as previously mentioned, the potent activities of both NAs against SARS-CoV-2 ExoN in its original wild type from the beginning prior to any intended mutations). These previous values of riboprine and forodesine even surpassed those of the two potent reference agents, remdesivir and molnupiravir, which showed higher values, reflecting the possible superiority of both NAs over remdesivir/molnupiravir in clinical investigation in humans. The results also proved that molnupiravir and remdesivir could

not resist the performance of Omicron variant ExoN the same way and potency as riboprine and forodesine do. The other target NAs, nelarabine, tecadenoson, maribavir, and vidarabine, also showed very good promising and small values but with less degree than those of riboprine, forodesine, and the reference molnupiravir, respectively. The TP nucleotides of the two top-ranked NAs in this assay, riboprine-TP and forodesine-TP, were also tested. Both nucleotides were very active against RdRp and ExoN enzymes, exhibiting slightly better activities as compared to their nucleosidic prodrugs and significantly better activities as compared to their reference TP nucleotidic drugs (GS-443902 and NHC-TP), but with little superiority of forodesine-TP over riboprine-TP, as demonstrated in Table 2. It is apparently observed from the values in Table 2 that the closer the EC₅₀ values of the NA/nucleotide analogue against the polymerase alone and against the polymerase in the presence of the exoribonuclease to each other, the more potent this NA/nucleotide analogue inhibitor (i.e., as more predicted for this tested analogue to be an ideally effective RdRp inhibitor or, more accurately, SARS-CoV-2 replication inhibitor). From the results, we can also conclude that an ideal potent SARS-CoV-2 RdRp inhibitor should have a ratio of EC₅₀(polymerase + exoribonuclease)/EC₅₀(polymerase) that is very close to 1 and less than 2. As this ratio decreases, as the compound has higher potential to succeed in inhibiting the SARS-CoV-2 replication more perfectly. Forodesine-TP and riboprine-TP, respectively, displayed the highest resistance, among all of the tested compounds, to the SARS-CoV-2 nsp14 exoribonuclease activity in HEK293T cells. The very promising capabilities of

riboptine/riboptine-TP and forodesine/forodesine-TP to inhibit the nsp12 polymerase and nsp14 exoribonuclease activities of the SARS-CoV-2 Omicron variant interestingly uphold the repurposing potentials of riboprine and forodesine along with their TP nucleotides in clinical settings for further therapeutic use as potent anti-COVID-19 drugs. It is worth mentioning that riboprine and forodesine are nearly the only NAs that have such unique potent anti-SARS-CoV-2 activities against both the RdRp and ExoN enzymes of the newest SARS-CoV-2 variant, Omicron variant, in very significant values to date (this is to the best of our current knowledge during the submission of this research paper for publication).^{24,25} These present biochemical findings concerning the potent inhibitory SARS-CoV-2 RdRp-binding and ExoN-binding properties of riboprine/riboptine-TP and forodesine/forodesine-TP are in ideal agreement with almost all of the computed parameters of the prior *in silico* part of this comprehensive research, which was discussed in detail in Section 3.1.

The second assay is the collective *in vitro* anti-SARS-CoV-2 and cytotoxicity tests. Table 3 shows the resulting values from both tests in detail. The used SARS-CoV-2 strain in the anti-SARS-CoV-2 assay is the new variant of SARS-CoV-2, the Omicron variant B.1.1.529.1/BA.1 sublineage, which is one of the most infectious and resistant strains of the virus. The data displayed in the table interestingly revealed the significantly higher antiviral efficacies of each of the two NAs riboprine and forodesine against the newly appeared variants of SARS-CoV-2 as compared to those of each of the two positive control reference drugs remdesivir and molnupiravir (the placebo drug DMSO showed extremely weak activities, i.e., negligible results). Riboprine and forodesine were found to efficiently inhibit and impair the entire SARS-CoV-2 replication/transcription in Vero E6 cells with EC_{50} values extremely smaller than the 100 μM value of stock concentration, continuing their superiorities over the other tested target NAs exactly as in the previous anti-RdRp/ExoN biochemical assay. Promisingly, natural NA riboprine was proved to be very leading (i.e., ranked first among all of the tested compounds) in its total anti-Omicron activity ($EC_{50} = 0.40 \mu\text{M}$), which was found to be about 5 and 6.5 times as effective as the two reference drugs remdesivir ($EC_{50} = 2.01 \mu\text{M}$) and molnupiravir ($EC_{50} = 2.60 \mu\text{M}$), respectively, with respect to the tested *in vitro* anti-B.1.1.529.1/BA.1/anti-SARS-CoV-2 activity, while forodesine was ranked second, among all of the tested compounds, in its total anti-Omicron activity ($EC_{50} = 0.65 \mu\text{M}$), which was found to be about 3.1 and 4 times as effective as the two reference drugs remdesivir and molnupiravir, respectively, with respect to the same evaluated activity. According to the current cytotoxicity assay, the *in vitro* CC_{50} values of riboprine and forodesine are significantly greater than 100 μM ; therefore, these two NAs are expected to have very advantageous high corresponding clinical selectivity indices "SIs" ($SI_{\text{riboprine}} > 250$ and $SI_{\text{forodesine}} > 153.9$, while remdesivir and molnupiravir have narrower SIs, $SI_{\text{remdesivir}} > 49.8$ and $SI_{\text{molnupiravir}} > 38.5$), reflecting the specific/selective anti-RNA actions of the riboprine and forodesine molecules against the new SARS-CoV-2 Omicron genome rather than the human genome. Riboprine and forodesine displayed significantly small values of the concentration that results in 100% *in vitro* inhibition of the SARS-CoV-2 Omicron variant cytopathic effects ($CPEIC_{100} = 1.08$ and $1.58 \mu\text{M}$, respectively), which are less than the corresponding values of remdesivir ($CPEIC_{100} =$

$5.90 \mu\text{M}$) and molnupiravir ($CPEIC_{100} = 6.24 \mu\text{M}$) and also less than those of the other tested NAs. In line with their potent activities against the infectious SARS-CoV-2 B.1.1.529.1/BA.1 strain, riboprine and forodesine also showed very low values of the concentration that is needed for 50% *in vitro* lowering in the number of RNA copies of the B.1.1.529.1/BA.1 strain of SARS-CoV-2 (0.42 and 0.69 μM , respectively), which are clearly smaller than the corresponding values of both remdesivir and molnupiravir (2.08 and 2.71 μM , respectively). EC_{90} values for riboprine and forodesine, which are preferably used for the *in vivo*/clinical studies, were also very small and consistent with the EC_{50} values (being not far that much from the EC_{50} values indicates the expected significant clinical potencies of both drugs), as demonstrated in Table 3. Nelarabine, tecadenoson, maribavir, and vidarabine displayed slightly higher concentration values (EC_{50} , EC_{90} , CC_{50} , and $CPEIC_{100}$) than those displayed by riboprine and forodesine but still comparable to those of the positive control drugs remdesivir and molnupiravir. Exactly as in the previous assay, the TP nucleotides of the two top-ranked NAs in this second assay, riboprine-TP and forodesine-TP, were also examined. Both nucleotides were very active against SARS-CoV-2 Omicron variant particles, exhibiting slightly better activities as compared to their nucleosidic prodrugs and significantly better activities as compared to their reference TP nucleotidic drugs (GS-443902 and NHC-TP) but with little superiority of forodesine-TP over riboprine-TP, as shown in Table 3. Being very biocompatible TP esters, forodesine-TP and riboprine-TP displayed acceptable cytotoxicities ($CC_{50} > 100 \mu\text{M}$).

The data of the *in vitro* anti-SARS-CoV-2 assay surprisingly reflected the relatively rapid mode of action of riboprine and forodesine against the SARS-CoV-2 Omicron variant particles. The current results of this reliable bioassay are in excellent agreement with almost all of the findings of the previous anti-RdRp biochemical assay along with the previous computational study (which was discussed in detail in Section 3.1) of this current comprehensive research.

The previous experimental findings significantly support our hypothesis that the top-ranked NAs in this current work, riboprine and forodesine, may exert their potent anti-SARS-CoV-2 activities either directly as noncovalent ligands (inhibitors) of the SARS-CoV-2 major replication enzymes, e.g., the RdRp/ExoN proteins, or indirectly as nucleosidic prodrugs that are principally *in vivo* metabolized into their TP nucleotidic forms, riboprine-TP and forodesine-TP (they are pharmacokinetically known to be the major final phosphorylated metabolites of both drugs), that are in turn covalently incorporated in the newly growing SARS-CoV-2 RNA strands in place of the structurally similar endogenous/natural TP nucleotides, e.g., ATP, through deceiving the replication enzymes, causing lethal mutagenesis of the about-to-be-generated SARS-CoV-2 particles.

Recently, nucleoside/nucleotide antivirals topped the scene as the first and early choices for COVID-19 therapy.³⁶ Riboprine is a natural purine nucleoside analogue (mainly a phytochemical metabolite/plant hormone) investigated for its potential various antineoplastic/antiproliferative, proapoptotic, neuroprotective, and antiangiogenic activities,³⁷ while forodesine is a very potent synthetic and unique highly selective transition-state analogue inhibitor of purine nucleoside phosphorylase (PNP), approved and used recently for the effective treatment of relapsed/refractory peripheral T-cell lymphoma.³⁸ Accordingly, being anticancer agents, the slight

host cytotoxic side effects and other possible adverse effects of riboprine and forodesine should be put into consideration and monitored during the clinical trials against COVID-19 to ensure that they do not outweigh the therapeutic benefits. These potential side effects can be effectively prevented by making use of the targeted drug delivery formulation techniques. It is worth mentioning that a recent study, about the riboprine repurposing potential for COVID-19 therapy, was published in 2021 by Bakowski and co-workers in *Nature Communications* journal during the preparation and processing of our current research work.³⁹ The findings of this study partially highlighted the high potency of this drug against SARS-CoV-2 particles *in vitro* in human lung epithelial cell lines, especially if riboprine was combined with remdesivir.³⁹ Interestingly, synergistic drug combination therapy has the significant possibility of boosting the effectiveness of treatment while slowing drug resistance acquisition as well as decreasing the drug dose of either or both/all integration partners, and therefore this combination therapy reduces and prevents side/adverse effects that may arise from administration of higher doses of a single drug, especially in the case of repurposed cytotoxic/anticancer agents. This combination therapy protocol can provide another potential solution for preventing the aforementioned side effects that may be associated with administration of the unphosphorylated prodrugs riboprine and forodesine as monotherapies.

Physically, riboprine and forodesine molecules have very flexible chemical structures that can easily tolerate chemical changes in biological systems. It was clearly found in the current research study that SARS-CoV-2 particles are very sensitive to both compounds and thoroughly mutated/inhibited by them. Interestingly, it was discovered that riboprine and forodesine may effectively stop SARS-CoV-2 spreadability and pathogenicity (and, consequently, end COVID-19 infection as a whole) in the human body, mainly through severely hindering SARS-CoV-2 replication *via* a double synergistic inhibitory mode of action against the two SARS-CoV-2 enzymes RdRp and ExoN. This double mode of action could be extended to a triple one if the expected inhibitory effects of the two drugs against kinases, especially on adenosine kinase (ADK), are extensively explored and proved in a next study. Similar to their natural analogues, the TP esters (the end active metabolites) of riboprine and forodesine are predicted to be as effective as the administered original prodrugs since they showed very encouraging anti-SARS-CoV-2 EC₅₀ values of 0.39 and 0.38 μM , respectively. Accordingly, the current work also revealed that these two nucleosidic prodrugs, forodesine and riboprine, may also exert their strong *in vivo* anti-SARS-CoV-2 activities *via* their corresponding final active metabolites, the TP nucleotide analogues forodesine-TP and riboprine-TP, respectively.

4. CONCLUSIONS

The current comprehensive *in silico/in vitro* preclinical research study detected the anti-COVID-19 potentials of a series of NAs, with riboprine and forodesine being the most promising potent SARS-CoV-2 RNA mutagens (mainly through their TP nucleotides) or, at least, the most promising SARS-CoV-2 replication inhibitors in general. Based on the current research observations, the two NAs, riboprine and forodesine, are specifically prioritized as prospective COVID-19 therapeutic drugs (with very promising anti-SARS-CoV-2 EC₅₀ values of 0.40 and 0.65 μM , respectively, against the Omicron variant),

while all of the six promising NAs, riboprine, forodesine, nelarabine, tecadenoson, maribavir, and vidarabine, generally warrant deeper pharmacological and clinical investigations to clearly understand their accurate therapeutic values as potential anti-SARS-CoV-2 agents.

AUTHOR INFORMATION

Corresponding Authors

Amgad M. Rabie – Dr. Amgad Rabie's Research Lab. for Drug Discovery (DARLD), Mansoura City 35511, Mansoura, Dakahlia Governorate, Egypt; Head of Drug Discovery & Clinical Research Department, Dikernis General Hospital (DGH), Dikernis City 35744, Dikernis, Dakahlia Governorate, Egypt; orcid.org/0000-0003-3681-114X; Phone: 002-01019733188; Email: amgadpharmacist1@yahoo.com, dr.amgadrabie@gmail.com

Mohnad Abdalla – Key Laboratory of Chemical Biology (Ministry of Education), Department of Pharmaceutics, School of Pharmaceutical Sciences, Cheeloo College of Medicine, Shandong University, Jinan, Shandong Province 250012, P. R. China; orcid.org/0000-0002-1682-5547; Email: mohnadabdalla200@gmail.com

Complete contact information is available at:

<https://pubs.acs.org/10.1021/acsbiochemau.2c00039>

Author Contributions

CRediT: **Amgad M. Rabie** conceptualization (lead), data curation (lead), formal analysis (lead), investigation (lead), methodology (lead), project administration (lead), resources (lead), software (equal), supervision (lead), validation (lead), visualization (equal), writing-original draft (lead), writing-review & editing (lead); **Mohnad Abdalla** software (equal), visualization (equal).

Notes

The authors declare no competing financial interest. Almost all of the produced computational and biological data relevant to this research work were already properly reported in this present research paper. The authors hereby declare that they totally have no known competing financial interests or personal relationships that could have appeared to influence the work reported in this new research paper.

ACKNOWLEDGMENTS

This new discovery did not receive any external funding. The authors gratefully thank and deeply acknowledge anyone who helped to make this new discovery and work coming out to light.

REFERENCES

- (1) Chitalia, V. C.; Munawar, A. H. A painful lesson from the COVID-19 pandemic: the need for broad-spectrum, host-directed antivirals. *J. Transl. Med.* **2020**, *18*, No. 390.
- (2) Wang, X.; Cao, R.; Zhang, H.; Liu, J.; Xu, M.; Hu, H.; Li, Y.; Zhao, L.; Li, W.; Sun, X.; Yang, X.; Shi, Z.; Deng, F.; Hu, Z.; Zhong, W.; Wang, M. The anti-influenza virus drug, arbidol is an efficient inhibitor of SARS-CoV-2 *in vitro*. *Cell Discovery* **2020**, *6*, No. 28.
- (3) Kaur, H.; Sarma, P.; Bhattacharyya, A.; Sharma, S.; Chhimpia, N.; Prajapat, M.; Prakash, A.; Kumar, S.; Singh, A.; Singh, R.; Avti, P.; Thota, P.; Medhi, B. Efficacy and safety of dihydroorotate dehydrogenase (DHODH) inhibitors "Ieflunomide" and "terifluno-

- midé" in Covid-19: A narrative review. *Eur. J. Pharmacol.* **2021**, *906*, No. 174233.
- (4) Rabie, A. M. Teriflunomide: A possible effective drug for the comprehensive treatment of COVID-19. *Curr. Res. Pharmacol. Drug Discovery* **2021**, *2*, No. 100055.
- (5) Rabie, A. M. Cyanorona-20: The first potent anti-SARS-CoV-2 agent. *Int. Immunopharmacol.* **2021**, *98*, No. 107831.
- (6) Ip, A.; Ahn, J.; Zhou, Y.; Goy, A. H.; Hansen, E.; Pecora, A. L.; Sinclaire, B. A.; Bednarz, U.; Marafelias, M.; Sawczuk, I. S.; Underwood, J. P., III; Walker, D. M.; Prasad, R.; Sweeney, R. L.; Ponce, M. G.; La Capra, S.; Cunningham, F. J.; Calise, A. G.; Pulver, B. L.; Ruocco, D.; Mojares, G. E.; Eagan, M. P.; Ziontz, K. L.; Mastrokyriakos, P.; Goldberg, S. L. Hydroxychloroquine in the treatment of outpatients with mildly symptomatic COVID-19: a multi-center observational study. *BMC Infect. Dis.* **2021**, *21*, No. 72.
- (7) Tardif, J.-C.; Bouabdallaoui, N.; L'Allier, P. L.; Gaudet, D.; Shah, B.; Pillinger, M. H.; Lopez-Sendon, J.; Da Luz, P.; Verret, L.; Audet, S.; Dupuis, J.; Denault, A.; Pelletier, M.; Tessier, P. A.; Samson, S.; Fortin, D.; Tardif, J.-D.; Busseuil, D.; Goulet, E.; Lacoste, C.; Dubois, A.; Joshi, A. Y.; Waters, D. D.; Hsue, P.; Lepor, N. E.; Lesage, F.; Sainuret, N.; Roy-Clavel, E.; Bassevitch, Z.; Orfanos, A.; Stamatescu, G.; Grégoire, J. C.; Busque, L.; Lavallée, C.; Héту, P.-O.; Paquette, J.-S.; Deftereos, S. G.; Levesque, S.; Cossette, M.; Nozza, A.; Chabot-Blanchet, M.; Dubé, M.-P.; Guertin, M.-C.; Boivin, G.; for the COLCORONA Investigators. Colchicine for community-treated patients with COVID-19 (COLCORONA): a phase 3, randomised, double-blinded, adaptive, placebo-controlled, multicentre trial. *Lancet Respir. Med.* **2021**, *9*, 924–932.
- (8) Mahase, E. Covid-19: Pfizer's paxlovid is 89% effective in patients at risk of serious illness, company reports. *BMJ* **2021**, *375*, No. n2713.
- (9) Imran, M.; Kumar Arora, M.; Asdaq, S. M. B.; Khan, S. A.; Aqel, S. I.; Alshammari, M. K.; Alshehri, M. M.; Alshrari, A. S.; Mateq Ali, A.; Al-shammeri, A. M.; Alhazmi, B. D.; Harshan, A. A.; Alam, M. T.; Abida. Discovery, Development, and Patent Trends on Molnupiravir: A Prospective Oral Treatment for COVID-19. *Molecules* **2021**, *26*, No. 5795.
- (10) Moirangthem, D. S.; Surbala, L. Remdesivir (GS-5734) in COVID-19 Therapy: The Fourth Chance. *Curr. Drug Targets* **2021**, *22*, 1346–1356.
- (11) Yan, V. C.; Muller, F. L. Advantages of the Parent Nucleoside GS-441524 over Remdesivir for Covid-19 Treatment. *ACS Med. Chem. Lett.* **2020**, *11*, 1361–1366.
- (12) Brunotte, L.; Zheng, S.; Mecate-Zambrano, A.; Tang, J.; Ludwig, S.; Rescher, U.; Schloer, S. Combination Therapy with Fluoxetine and the Nucleoside Analog GS-441524 Exerts Synergistic Antiviral Effects against Different SARS-CoV-2 Variants In Vitro. *Pharmaceutics* **2021**, *13*, No. 1400.
- (13) Rabie, A. M. Potent Inhibitory Activities of the Adenosine Analogue Cordycepin on SARS-CoV-2 Replication. *ACS Omega* **2022**, *7*, 2960–2969.
- (14) Rabie, A. M. Efficacious Preclinical Repurposing of the Nucleoside Analogue Didanosine against COVID-19 Polymerase and Exonuclease. *ACS Omega* **2022**, *7*, 21385–21396.
- (15) Cai, Q.; Yang, M.; Liu, D.; Chen, J.; Shu, D.; Xia, J.; Liao, X.; Gu, Y.; Cai, Q.; Yang, Y.; Shen, C.; Li, X.; Peng, L.; Huang, D.; Zhang, J.; Zhang, S.; Wang, F.; Liu, J.; Chen, L.; Chen, S.; Wang, Z.; Zhang, Z.; Cao, R.; Zhong, W.; Liu, Y.; Liu, L. Experimental Treatment with Favipiravir for COVID-19: An Open-Label Control Study. *Engineering* **2020**, *6*, 1192–1198.
- (16) Rabie, A. M. Two antioxidant 2,5-disubstituted-1,3,4-oxadiazoles (CoViTris2020 and ChloViD2020): successful repurposing against COVID-19 as the first potent multitarget anti-SARS-CoV-2 drugs. *New J. Chem.* **2021**, *45*, 761–771.
- (17) Rabie, A. M. CoViTris2020 and ChloViD2020: a striking new hope in COVID-19 therapy. *Mol. Divers.* **2021**, *25*, 1839–1854.
- (18) Rabie, A. M. Potent toxic effects of Taroxaz-104 on the replication of SARS-CoV-2 particles. *Chem.-Biol. Interact.* **2021**, *343*, No. 109480.
- (19) Rabie, A. M. Discovery of Taroxaz-104: The first potent antidote of SARS-CoV-2 VOC-202012/01 strain. *J. Mol. Struct.* **2021**, *1246*, No. 131106.
- (20) Chien, M.; Anderson, T. K.; Jockusch, S.; Tao, C.; Li, X.; Kumar, S.; Russo, J. J.; Kirchoerfer, R. N.; Ju, J. Nucleotide Analogues as Inhibitors of SARS-CoV-2 Polymerase, a Key Drug Target for COVID-19. *J. Proteome Res.* **2020**, *19*, 4690–4697.
- (21) <https://www.who.int/en/activities/tracking-SARS-CoV-2-variants> (last accessed June 2, 2022).
- (22) <https://www.washingtonpost.com/health/2021/12/16/omicron-variant-mutations-covid/> (last accessed June 2, 2022).
- (23) Khater, S.; Kumar, P.; Dasgupta, N.; Das, G.; Ray, S.; Prakash, A. Combining SARS-CoV-2 Proofreading Exonuclease and RNA-Dependent RNA Polymerase Inhibitors as a Strategy to Combat COVID-19: A High-Throughput *in silico* Screening. *Front. Microbiol.* **2021**, *12*, No. 647693.
- (24) Zhao, J.; Liu, Q.; Yi, D.; Li, Q.; Guo, S.; Ma, L.; Zhang, Y.; Dong, D.; Guo, F.; Liu, Z.; Wei, T.; Li, X.; Cen, S. 5-Iodotubercidin inhibits SARS-CoV-2 RNA synthesis. *Antiviral Res.* **2022**, *198*, No. 105254.
- (25) Zhao, J.; Guo, S.; Yi, D.; Li, Q.; Ma, L.; Zhang, Y.; Wang, J.; Li, X.; Guo, F.; Lin, R.; Liang, C.; Liu, Z.; Cen, S. A cell-based assay to discover inhibitors of SARS-CoV-2 RNA dependent RNA polymerase. *Antiviral Res.* **2021**, *190*, No. 105078.
- (26) Lin, X.; Liang, C.; Zou, L.; Yin, Y.; Wang, J.; Chen, D.; Lan, W. Advance of structural modification of nucleosides scaffold. *Eur. J. Med. Chem.* **2021**, *214*, No. 113233.
- (27) Eissa, I. H.; Khalifa, M. M.; Elkaeed, E. B.; Hafez, E. E.; Alsouk, A. A.; Metwaly, A. M. *In Silico* Exploration of Potential Natural Inhibitors against SARS-Cov-2 nsp10. *Molecules* **2021**, *26*, No. 6151.
- (28) Wang, Y.; Chen, L. Tissue distributions of antiviral drugs affect their capabilities of reducing viral loads in COVID-19 treatment. *Eur. J. Pharmacol.* **2020**, *889*, No. 173634.
- (29) Doharey, P. K.; Singh, V.; Gedda, M. R.; Sahoo, A. K.; Varadwaj, P. K.; Sharma, B. *In silico* study indicates antimalarials as direct inhibitors of SARS-CoV-2-RNA dependent RNA polymerase. *J. Biomol. Struct. Dyn.* **2022**, *40*, 5588–5605.
- (30) RdRp. Available from DrugDevCovid19, http://clab.labshare.cn/covid/php/database_target.php?target=RdRp&id=P0DDTD1 (last accessed June 6, 2022).
- (31) Moeller, N. H.; Shi, K.; Demir, Ö.; Belica, C.; Banerjee, S.; Yin, L.; Durfee, C.; Amaro, R. E.; Aihara, H. Structure and dynamics of SARS-CoV-2 proofreading exonuclease ExoN. *Proc. Natl. Acad. Sci. U. S. A.* **2022**, *119*, No. e2106379119.
- (32) Nsp14. Available from DrugDevCovid19, http://clab.labshare.cn/covid/php/database_target.php?target=nsp14&id=P0DDTD1 (last accessed June 7, 2022).
- (33) Smith, E. C.; Blanc, H.; Surdel, M. C.; Vignuzzi, M.; Denison, M. R. Coronaviruses Lacking Exoribonuclease Activity Are Susceptible to Lethal Mutagenesis: Evidence for Proofreading and Potential Therapeutics. *PLoS Pathog.* **2013**, *9*, No. e1003565.
- (34) Ferron, F.; Subissi, L.; Silveira De Morais, A. T.; Le, N. T. T.; Sevajol, M.; Gluais, L.; Decroly, E.; Vonnrhein, C.; Bricogne, G.; Canard, B.; Imbert, I. Structural and molecular basis of mismatch correction and ribavirin excision from coronavirus RNA. *Proc. Natl. Acad. Sci. U. S. A.* **2018**, *115*, E162–E171.
- (35) Hillen, H. S.; Kokic, G.; Farnung, L.; Dienemann, C.; Tegunov, D.; Cramer, P. Structure of replicating SARS-CoV-2 polymerase. *Nature* **2020**, *584*, 154–156.
- (36) Jockusch, S.; Tao, C.; Li, X.; Anderson, T. K.; Chien, M.; Kumar, S.; Russo, J. J.; Kirchoerfer, R. N.; Ju, J. A library of nucleotide analogues terminate RNA synthesis catalyzed by polymerases of coronaviruses that cause SARS and COVID-19. *Antiviral Res.* **2020**, *180*, No. 104857.
- (37) Riboprine. PubChem CID: 24405. Available from PubChem, <https://pubchem.ncbi.nlm.nih.gov/compound/Riboprine> (last accessed July 13, 2022).
- (38) Kicska, G. A.; Long, L.; Hörig, H.; Fairchild, C.; Tyler, P. C.; Furneaux, R. H.; Schramm, V. L.; Kaufman, H. L. Immucillin H, a

powerful transition-state analog inhibitor of purine nucleoside phosphorylase, selectively inhibits human T lymphocytes. *Proc. Natl. Acad. Sci. U. S. A.* **2001**, *98*, 4593–4598.

(39) Bakowski, M. A.; Beutler, N.; Wolff, K. C.; Kirkpatrick, M. G.; Chen, E.; Nguyen, T.-T. H.; Riva, L.; Shaabani, N.; Parren, M.; Ricketts, J.; Gupta, A. K.; Pan, K.; Kuo, P.; Fuller, M.; Garcia, E.; Teijaro, J. R.; Yang, L.; Sahoo, D.; Chi, V.; Huang, E.; Vargas, N.; Roberts, A. J.; Das, S.; Ghosh, P.; Woods, A. K.; Joseph, S. B.; Hull, M. V.; Schultz, P. G.; Burton, D. R.; Chatterjee, A. K.; McNamara, C. W.; Rogers, T. F. Drug repurposing screens identify chemical entities for the development of COVID-19 interventions. *Nat. Commun.* **2021**, *12*, No. 3309.